UNIVERSITÀ DEGLI STUDI DI PADOVA
DIPARTIMENTO DI INGEGNERIA CIVILE, EDILE E AMBIENTALE
Department of Civil, Environmental and Architectural Engineering

Corso di Laurea Magistrale in Environmental Engineering

MASTER THESIS

Strategic Market Participation of an Energy Storage System in a Competitive Electricity Market Considering Short-run Uncertainties

Supervisor:

PROF.SSA MARIA CRISTINA LAVAGNOLO

Student:

SOHEIL ABED (2004939)

Academic Year 2022-2023

I dedicate this thesis to Kian Pir Falak, a bright 9-year-old who was tragically killed during antigovernment protests in Iran. Kian dreamed of working at NASA, and his potential was cut short by senseless violence. May his memory inspire us to work towards a better world where such tragedies never happen again.

“Woman, Life, Freedom”

ACKNOWLEDGEMENT

I would like to express my heartfelt gratitude to my family and friends who have been my constant support throughout my academic journey. Their love, encouragement, and unwavering belief in me have been a source of strength and motivation.

I am also grateful to Professor Lavagnolo and Professor Shariat for their guidance, encouragement, and valuable feedback throughout my thesis research. Their expertise, insights, and willingness to challenge my ideas have been invaluable in shaping my research.

Abstract

This thesis proposes an efficient method for scheduling and operating a power system with a single storage unit. The method utilizes a market clearing mechanism that incorporates distributed robust chance constraint (DRCC) methods to manage the risk associated with uncertain flexible technologies. The study assumes a fully centralized market setup and aims to optimize utility within the power sector while accounting for the presence of a storage system. The approach assumes an affine response to uncertainty, enabling the market operator to identify the most effective plan for executing flexibility to maximize social welfare in the day-ahead market and manage potential power imbalances in real-time operations. The dispatch mechanism takes into account the "availability costs" of flexible assets to manage their utilization efficiently. The study demonstrates that the proposed method enhances social welfare by taking advantage of the synergies between interconnected power networks and storage, particularly in situations where renewable energy generation is uncertain. However, the model is sensitive to the choice of price differences, availability costs, and investment costs, and cannot precisely advise building an energy storage system to provide flexibility response.

Table of Contents

1. Introduction

1.1 General Background

In recent years, the energy sector has experienced several challenges, including the depletion of conventional energy resources and the aging of electrical network infrastructure (Azari et al., 2019; Ramos et al., 2016). The energy system as we know it today is undergoing a significant transformation, commonly called the energy transition (Wiseman, 2018). This transformation encompasses rapid structural changes in energy production, distribution, and consumption at all levels and is driven by three main pillars: decarbonization, decentralization, and digitalization (di Silvestre et al., 2018; Geels, 2002; Gritsenko, 2018).

Decarbonization represents a shift from an energy system dominated by fossil fuels to an energy system based primarily on renewable energy resources (RES). While RES technologies, such as wind and solar farms, hold tremendous potential for reducing greenhouse gas emissions, their production profile is highly variable and challenging to forecast accurately, even in the short term (Azari et al., 2020). Decentralization involves increased customer participation in energy demand management and consumer empowerment, particularly at the distribution level (di Silvestre et al., 2018; Geels, 2002; Gritsenko, 2018). Meanwhile, digitalization encompasses the development of new energy and service exchange paradigms and the widespread implementation of data-driven, software-powered energy management technologies in urban environments (di Silvestre et al., 2018; Geels, 2002; Gritsenko, 2018).

Given these challenges, the integration of RES into power networks has been proposed as a solution to the increasing uncertainty in the energy system. However, this integration also increases the level of uncertainty in the energy value chain, making the planning and operation of power systems more challenging (Godoy Simões et al., 2014). As a result, system operators (SOs) need to use available flexibility more effectively and cost-effectively to deal with the increased renewable energy (Torbaghan et al., 2018).

Increasing the flexibility in power systems is one possible solution to mitigate this uncertainty. Flexibility can be achieved through various means, including energy storage, sector integration (such as gas-electricity or water-electricity), demand-response services, and expanding the geographical scope of the energy system (Oconnell et al., 2014; Shariat Torbaghan et al., 2021; Torbaghan et al., 2020). Furthermore, the decentralization and digitalization of energy systems can increase energy efficiency through lower investment and operational costs and a higher degree of autonomy for individual energy participants, particularly in power systems (Ordoudis et al., 2019).

Efforts have been made to deal with the emerging uncertainties in the energy system by harnessing the operational flexibility of prosumers (proactive electricity consumers who can also produce, share, or store energy). This has led to a shift towards a more bottom-up, consumer-centric approach to energy systems (Ratha et al., 2020).

In the power system, various local energy trading platforms have been developed, including centralized (Mitridati et al., 2020; Schwele et al., 2020), decentralized (Alskaif et al., 2022; Mengelkamp et al., 2018; van Leeuwen et al., 2020), and distributed (le Cadre et al., 2020; Sorin et al., 2018; Tushar et al., 2020) platforms. These advances in technology and energy management can improve the energy system's reliability, efficiency, and sustainability in the years to come.

1.2 Problem statement (The Challenge)

The field of energy storage involves two types of planning: investment (reinforcement) planning and operational (scheduling) planning. It is important to note that the storage capacity is fixed in operational planning, while in investment planning, it is considered unknown. It is necessary first to resolve the operational planning issue to address the challenges posed by energy storage.

This thesis focuses on the use of flexible technologies. It aims to provide a solution for investigating and managing the uncertainty associated with scheduling an energy storage system in a power system. The scheduling of energy storage systems plays a crucial role in ensuring a power system's efficient and effective operation. The integration of energy storage technologies introduces uncertainty that must be considered in the planning and scheduling processes (Li, Cheng, & Liu, 2016).

This thesis aims to advance the understanding of energy storage and provide practical insights into the effective integration of energy storage technologies into power systems. The focus on scheduling energy storage systems and the proposed solution for addressing uncertainty will support the development of more efficient and effective energy storage systems.

In conclusion, scheduling energy storage systems in a power system is a crucial aspect of ensuring efficient and effective energy storage. Integrating energy storage technologies introduces uncertainty that must be considered in the planning and scheduling processes. This thesis focuses on using flexible technologies and proposes a solution for investigating and managing the uncertainty associated with scheduling energy storage systems in a power system.

1.3 Research Aim

The present study endeavors to advance the state-of-the-art in modeling power systems under uncertainty. Against the backdrop of an ever-evolving power grid landscape, this thesis addresses the challenge of incorporating storage capacity into power system models in the face of uncertainty.

This study's central research question will explore the feasibility of developing a robust method for modeling a power grid with storage capacity that considers the various distribution possibilities in an uncertain environment. The thesis will seek to answer this question by focusing on several vital sub-questions, which will be tackled through a comprehensive and systematic investigation, which are as follows:

1. What does the wind power uncertainty look like?
2. How can uncertainty be modeled?
3. What methodologies enable us to consider the case with non-probability distributions?

In light of the increasing importance of power grids with storage capacity, it is crucial to establish a better understanding of how to model these systems under uncertainty. The results of this study are expected to contribute to the broader literature on power system modeling and provide valuable insights for practitioners in the field.

2. Materials and methods

The increasing presence of uncertainty in the power system presents a significant challenge for market and system operators. With the growing integration of variable renewable energy sources and the unpredictable nature of demand, the likelihood of expensive rapid-response equipment activation and offload events is on the rise. To mitigate this risk, it is essential to ensure that there is a sufficient reserve of generating capacity to accommodate sudden fluctuations in the system. Unfortunately, the current deterministic market-clearing approach fails to account for the random behavior of these new participants, resulting in inefficient allocations (Morales et al., 2014).

The power system is subject to a significant degree of uncertainty, which may result in costly rapid response equipment activation and offload events. The likelihood of such occurrences is expected to increase in the future due to the rising use of variable renewable energy sources and unpredictable demand. To mitigate this risk, system, and market operators must ensure that they have sufficient generating capacity in reserve to manage unexpected fluctuations. However, the current deterministic approach to market clearing fails to account for the stochastic nature of these new participants, leading to suboptimal allocations (Morales et al., 2014).

This highlights the need for new methods to address the challenges posed by uncertainty in the power system. Some proposed solutions include stochastic optimization and robust optimization models (Papavasiliou et al., 2015; Rostami et al., 2021). These models aim to incorporate uncertainty into the optimization process and provide more robust decision-making frameworks. Another approach is the use of demand response programs, which incentivize consumers to reduce their energy usage during periods of high demand or low supply (Siano, 2014). Such programs can help balance the system and reduce the need for expensive rapid response equipment activation. Overall, a combination of these approaches may be necessary to effectively manage the growing uncertainty in the power system.

In this section, we aim to explore these recommended techniques for handling high levels of uncertainty in the power system through the market clearing mechanism. To provide a comprehensive analysis, we will examine the mathematical formulation of the problem, including the power system and storage constraints, which play a critical role in ensuring the stability and reliability of the power system. Further research in this area could include a more in-depth analysis of the market clearing mechanisms in different regions and a comparison of the advantages and disadvantages of each approach.

2.1 Literature review

2.1.1 Stochastic Programming

The stochastic programming approach is a mathematical modeling technique that has been proposed to effectively manage uncertainty in the power system. The presence of a significant amount of uncertainty in the power system increases the likelihood of expensive rapid response equipment activation and offload events occurring. This aspect is expected to be even more relevant in the future, given the growing penetration of variable renewable energy sources and uncertain demand. To mitigate this risk, the system and market operators must ensure that sufficient generating capacity is in reserve dynamically to deal with unexpected fluctuations. However, the current deterministic approach to market clearing does not take into account the random nature of these new participants, which can lead to inefficient allocations (Morales et al., 2014).

The two-step SP approach aims to minimize expected system operating costs by considering both energy and labor costs associated with market allocation, reserve capacity (stage 1), and the expected cost of actual adjustment actions, such as load-shedding or renewable energy source reduction decisions (stage 2) (Morales et al., 2014). The approach represents the production of variable renewable energy sources as uncertainty and uses a set of scenarios to reflect the probabilities of different scenarios and their associated costs.

In the SP approach, several constraints are also taken into consideration, such as energy balance equations for the DA market, real-time balance, bounds on submitted bids, non-negative variables, and limits associated with load shedding, curtailment, and reserve activation (Papavasiliou & Oren, 2014). The SP model has been shown to have several benefits, including better performance than the conventional economic dispatch (ED) model and a reduction of market power and price volatility due to the aggregation of large volumes of transactions through the co-optimization of the DA and balancing authority (BA) markets (Conejo et al., 2012).

However, the SP model is not without its limitations. Despite several attempts to fill the gap in SP modeling, the high computational burden created by a large number of scenarios remains a challenge, resulting in increased system costs (López et al., 2021). Additionally, the model's reliance on an accurate representation of uncertainty can be problematic if the underlying data is unreliable (Wu et al., 2019). Despite these drawbacks, the SP model remains a promising approach for managing uncertainty in the power system.

2.1.2 Chance Constraint Optimization

The field of energy management has seen a growing interest in the use of chance constraint optimization (CCO) as a tool to mitigate the risks posed by uncertainty in the power system. In comparison to scenario-based stochastic programming (SP) models, CCO offers a way to explicitly consider uncertainty variables within the optimization problem itself, by formulating

constraints that represent the probability space of the constraints, ensuring that operational boundaries are not violated within a specified confidence level.

The formulation of the chance constraints in CCO is a crucial aspect of this approach, as they are representations of random variables, often modeled using probability density functions, and corresponding to the errors associated with the variable renewable energy sources and load forecasting. The CCO approach has been applied to the economic dispatch of the day-ahead (DA) market, considering system reserve limits and transmission line limits as chance constraints.

The benefits of using CCO are numerous, as it provides a balance between reliability and economic efficiency, as less restrictive chance constraints lead to lower total costs in the DA market, while at the same time ensuring the reliability of the system operation. In particular, CCO has been shown to promote the efficient use of wind energy, while maintaining a high level of system reliability (Q. Wang et al., 2012; J. Wu et al., 2019).

However, the use of CCO is not without its limitations, as the complexity of the problem increases with the number of constraints formulated as chance constraints, leading to a point where meeting all constraints may become impossible and resulting in the convergence of the optimization problem (Y. Wang et al., 2017; H. Wu et al., 2014). Additionally, while CCO has been shown to perform better than conventional economic dispatch models, the higher computational burden associated with this approach can present a challenge in its implementation.

Chance constraint optimization involves incorporating probabilistic constraints into the optimization problem. The dimensionality of chance constraints is directly related to the number of uncertain parameters involved in the problem. As the number of uncertain parameters increases, the dimensionality of the problem also increases, making the optimization problem more computationally expensive. Several studies have explored methods to reduce the dimensionality of chance constraint optimization problems, such as using principal component analysis (PCA) to reduce the number of uncertain parameters or decomposing the problem into smaller sub-problems. These techniques can help reduce the computational burden of chance constraint optimization and make it more practical for real-world applications.

Despite these limitations, the use of CCO in the management of uncertainty in the power system is an area of active research and development, as the advantages of this approach offer promising results in the achievement of both economic efficiency and system reliability.

2.1.3 Robust Optimization

The robust optimization (RO) approach is a powerful tool for addressing uncertainty in the energy dispatch problem (Bertsimas et al., 2013; Jiang et al., 2012; Morales et al., 2014; Zugno & Conejo, 2015). This method is characterized by its focus on robustness, which refers to the

ability to meet a given requirement under the worst-case realization. By considering the most unfavorable conditions during the balancing stage, the RO approach aims to minimize the costs of dispatching energy.

Despite its potential benefits, the RO approach has been studied by only a limited number of researchers. Nevertheless, it can be said that the RO method provides a feasible solution for all possible values of the uncertain parameters and an optimal solution under the worst-case event (Hu et al., 2016; Jiang et al., 2013; Morales et al., 2014). Additionally, the RO approach can help minimize the likelihood of load-shedding events by ensuring that enough upward capacity is procured to deal with the worst-case scenario (Bertsimas et al., 2013; Jiang et al., 2012; Morales et al., 2014; Zugno & Conejo, 2015).

The Robust Optimization (RO) approach, despite being a valuable tool for addressing uncertainty in the energy dispatch problem and ensuring reliable and efficient energy systems (Bertsimas et al., 2013; Jiang et al., 2012; Morales et al., 2014; Zugno & Conejo, 2015), faces several limitations, with one of the most notable being its tendency towards conservatism. This conservativeness, particularly in terms of the provision of upward reserves, can result in significantly higher costs as compared to the current deterministic design (Jiang et al., 2013; Morales et al., 2014), which may be detrimental in certain circumstances. Nevertheless, the RO approach remains a crucial method for managing uncertainty in the energy dispatch problem and ensuring a robust and efficient energy system.

2.1.4 Distribution Robust Chance-Constraint

The presence of uncertainties, such as the variability of loads and renewable energy sources (RES) generation, has garnered significant attention in recent years due to their impact on energy systems. As forecasts for these uncertainties do not always reflect their actual real-time (RT) realization, it is crucial to consider them in demand-response mechanisms (Line et al., 2015; Pourahmadi & Kazempour, 2021).

Studies have shown that the errors resulting from imperfect forecasting algorithms are often not confined to a particular probability distribution, which is why traditional stochastic methods may not always provide an accurate solution (Line et al., 2015; Pourahmadi & Kazempour, 2021). This is where the Distribution Robust Chance-Constraint (DRCC) approach comes into play. The DRCC approach is highly valued in the energy dispatch field due to its ability to address uncertainties in a manner that is both less conservative and computationally efficient (Zakaria et al., 2020).

The DRCC approach offers several advantages compared to other stochastic methods as it does not require any assumptions on the probability distributions. This lack of constraint allows for a more flexible and adaptable solution to the problem at hand, leading to improved results and higher efficiency in real-world applications (Zakaria et al., 2020). In conclusion, the DRCC approach provides a valuable tool for mitigating the impact of uncertainties in energy dispatch, allowing for the maintenance of reliable and efficient energy systems.

2.2 Problem formulation

2.2.1 Modeling Assumptions

The underlying assumptions of the problem can be outlined as follows: it is postulated that the sole source of uncertainty in the model is the variation in wind power, and no other sources of uncertainty are considered. The probability distribution of the wind power deviation is assumed to be unknown, and therefore an ambiguity set is utilized to account for the uncertainty. By employing an ambiguity set, the range of possible values for the uncertain parameter is defined without specifying a specific probability distribution, thus allowing for greater flexibility in the model. This approach has been widely adopted in recent studies related to power systems with renewable energy sources, where uncertainties can have a significant impact on system performance (Deng et al., 2019; Zhu et al., 2019).

A single-area Power Transmission Network (PTN) is considered on the power side, which comprises a set of transmission lines L and nodes N, with each node containing uncontrollable loads l ∈ D, conventional power generating units e ∈ G, and wind generators w ∈ W. The power transmission network is modeled using a linearized DC optimal power flow (DC-OPF) formulation. The linear DC-OPF formulation assumes that voltage magnitudes are close to 1 per-unit and neglects power losses. Additionally, resistance is assumed to be small compared to reactance. Since voltage angle differences over the network elements are assumed to be small, the linear approximation can be used to model the sine function.

The DC-OPF formulation is widely used due to its simplicity and computational efficiency. However, it has certain limitations that need to be considered. One of the major limitations is the neglect of reactive power flows, which may not be negligible in certain situations, particularly in high voltage networks (Wang et al., 2020). Another limitation is the linearization of the power flow equations, which may not be accurate in systems with high penetration of renewable energy sources (Zhao et al., 2018). In addition, the DC-OPF formulation assumes that the network is in steady-state and does not take into account the dynamic behavior of the power system (Cai et al., 2016). Finally, the DC-OPF formulation may not accurately represent the physical constraints of the power system, such as thermal limits on transmission lines and voltage limits on buses (Nagy et al., 2019).

2.2.2 Mathematical formulation of the problem

The market clearing problem can be formulated as:

$$\underset{\Xi,\mathbb{P}\epsilon\Pi}{\text{Min}} \sum_{t\epsilon\mathcal{T}} \left[\left(\sum_{g\epsilon\mathcal{G}} q^{G}_{g,t} p^{G}_{g,t} - \sum_{d\epsilon\mathcal{D}} q^{D}_{d} p^{D}_{d,t} + \sum_{s\epsilon\mathcal{S}} p^{sprd}_{s} q^{ch}_{s,t} \right) + \sum_{g\epsilon\mathcal{G}} C^{Av}_{g} \alpha_{g,t} + \sum_{s\epsilon\mathcal{S}} C^{Av}_{s} \beta_{s,t} \right] \quad (1a)$$

As shown in the equation above, which is the objective function of the problem, the final goal of the model is to minimize the social cost and the cost oof the generators and the storage while charging and discharging. The equation (1a), is divided in to two main parts, first the ($\sum_{g\epsilon\mathcal{G}} q_{g,t}^{G} p_{g,t}^{G} - \sum_{d\epsilon\mathcal{D}} q_{d}^{D} p_{d,t}^{D} + \sum_{s\epsilon\mathcal{S}} p_{s}^{sprd} q_{s,t}^{ch}$) which is pointing to the social welfare which has been covered thoroughly in the Shariat Torbaghan et al., (2021) and second, the ($\sum_{g\epsilon\mathcal{G}} C_{g}^{Av} \alpha_{g,t} + \sum_{s\epsilon\mathcal{S}} C_{s}^{Av_{ch}} \beta_{s,t}^{ch} + \sum_{s\epsilon\mathcal{S}} C_{s}^{Av_{dc}} \beta_{s,t}^{dc}$) which is the replica of the former works of (Belmondo Bianchi et al., n.d.) the fact that in the aforementioned problem the part that corresponds to the water pumps has been replaced with two separate parts for the storages when charging and discharging.

As long as the first part of the objective model is the matter of concern it should be noted that the $q_{g,t}^{G}$ is the power production of the generator g at time t, $p_{g,t}^{G}$ is the price of the electricity generated by the generator g at time t, q_{d}^{D} is the quantity of power demand, $p_{d,t}^{D}$is the price of the power demand in the deterministic (day-ahead) market at time t, p_{s}^{sprd} represents an average cost or an average price spread to be recovered by the market participant to provide energy storage services as specified by the storage order and $q_{s,t}^{ch}$ is the quantity of power charging that takes place in the storage s at time t. It is important to know that when engaging in the act of purchasing a commodity for later resale or exchange in a different market, such as the purchase of electricity or natural gas for electricity production, the price difference between the initial purchase and subsequent sale is known as the spark spread (Bahadori et al., 2018). Conversely, the price difference between the initial purchase and later sale of a commodity like rice after a set period is known as the normal spread (Brorsen, 2013). It is important to note that a negative spread represents a financial loss, while a positive spread signifies a profitable transaction (Huang et al., 2021).

In electricity markets, price differences refer to variations in the cost of electricity across different times of the day or in different locations. These differences are primarily driven by changes in demand patterns, supply levels, fuel prices, and transmission constraints (Newbery, 2002). For instance, electricity prices may be higher during periods of peak demand, such as hot summer afternoons when air conditioners are running at full capacity. Similarly, price differences can also arise due to transmission constraints and differences in transmission costs across locations. Price differences in electricity markets provide an incentive for market participants to engage in arbitrage and trade electricity across locations or time periods, thereby helping to balance the supply and demand of electricity in the system They also play a crucial role in incentivizing investment in new generating capacity and transmission infrastructure (Joskow, 2012).

The dual variable associated with the power balance constraint (3i), determines the price of electricity, but only becomes available after the problem is solved (Vito, 2019). To make informed decisions about buying and selling electricity, it is necessary to have a forecast that indicates the expected price (Golshan et al., 2021). However, it is also important to evaluate the actual results against the forecast and adjust as needed. Alternatively, incorporating time-shifting orders (or storage orders) into the market could provide a better solution (Cao et al., 2020). This approach requires new communication protocols between market participants and

the market operator. Under this system, storage facilities would communicate their expected profit for each MW hour charged or discharged, rather than worrying about buy and sell prices (Cao et al., 2020). The market operator would clear the market and settle all relevant transactions based on the resulting price spreads (Cao et al., 2020). The first part of the objective function has been previously demonstrated in Vito's paper (Vito, 2019).

Regarding the second part of the objective function, C_g^{Av} is the average cost of the conventional generator power production, $\alpha_{g,t}$ is an auxiliary variable to express the cost of real-time service that generator g provides at time t, C_s^{Av} is the average cost of the storage s in the states of charging and discharging at time t, $\beta_{s,t}$ is the flexibility of storage s at time t (charging and discharging).

Constraints are an integral part of optimization problems, providing a means to incorporate limitations, objectives, and requirements into the solution. Constraints may be physical, operational, or regulatory, and serve to narrow down the solution space and ensure that the solution is feasible and realistic.

In engineering design problems, constraints can enforce performance, safety, or regulatory standards, while in resource allocation problems, they can limit the number of resources used. Constraints can also help to prevent overfitting in machine learning and ensure that the solutions generalize well to new data (Jordan et al., 2006). Overall, constraints play a critical role in optimization problems by enabling optimization algorithms to generate solutions that meet real-world constraints and requirements. In the subsequent sections of this segment, the power and storage constraints will be elaborated on 2.2.2.1 and 2.2.2.2 respectively.

2.2.2.1 Power Constraints

This section introduces and discusses the constraints associated with the power system. The limits for the generators, loads, and wind power are presented below.

$$\underset{\Xi,\mathbb{P}\epsilon\mathrm{II}}{\mathrm{Min}}\mathbb{P}\left[\hat{q}_{g,t}^{G}+(\phi^{T}\Delta w_t)\breve{q}_{g,t}^{G}\le\overline{Q}_{g}^{G}\right]\ge(1-\varepsilon) \qquad g\epsilon G,t\epsilon\mathcal{T} \qquad (1b)$$

$$\underset{\Xi,\mathbb{P}\epsilon\mathrm{II}}{\mathrm{Min}}\mathbb{P}\left[\hat{q}_{g,t}^{G}+(\phi^{T}\Delta w_t)\breve{q}_{g,t}^{G}\ge\underline{Q}_{g}^{G}\right]\ge(1-\varepsilon) \qquad g\epsilon G,t\epsilon\mathcal{T} \qquad (1c)$$

$$\underset{\Xi,\mathbb{P}\epsilon\mathrm{II}}{\mathrm{Min}}\mathbb{P}\left[\hat{f}_{n,m,t}+(\phi^{T}\Delta w_t)\breve{f}_{n,m,t}\le\overline{f}_{n,m,t}\right]\ge(1-\varepsilon) \qquad n\epsilon N,(n,m)\epsilon\mathcal{E}_n,t\epsilon\mathcal{T} \qquad (1d)$$

$$\underset{\Xi,\mathbb{P}\epsilon\mathrm{II}}{\mathrm{Min}}\mathbb{P}\left[\hat{f}_{n,m,t}+(\phi^{T}\Delta w_t)\breve{f}_{n,m,t}\ge\underline{f}_{n,m,t}\right]\ge(1-\varepsilon) \qquad n\epsilon N,(n,m)\epsilon\mathcal{E}_n,t\epsilon\mathcal{T} \qquad (1e)$$

$$\underline{Q}_{d}^{D}\le q_{d,t}^{D}\le\overline{Q}_{d}^{D} \qquad d\epsilon\mathcal{D} \qquad (1f)$$

$$\underline{Q}_{w}^{W}\le\tilde{q}_{d,t}^{W}\le\overline{Q}_{w}^{W} \qquad w\epsilon W \qquad (1g)$$

$$\alpha_{g,t}=(\phi^{T}\Delta w_t)\breve{q}_{g,t} \qquad g\epsilon G,t\epsilon\mathcal{T} \qquad (1h)$$

$$\sum_{g\epsilon\psi G_n} \hat{q}^{G}_{e,t} + \sum_{w\epsilon\psi W_n} \hat{q}^{W}_{w,t} + \sum_{s\epsilon\psi S_n} \hat{q}^{dc}_{s,t}\,\eta^{dc}_{s,t} = \sum_{d\epsilon\psi D_n} \hat{q}^{D}_{d,t} + \sum_{s\epsilon\psi S_n} \hat{q}^{ch}_{s,t} + \sum_{m\epsilon\Omega_n} \hat{q}_{n,m,t} \qquad n\epsilon N, t\epsilon\mathcal{T} \qquad (1i)$$

$$\sum_{g\epsilon G} \breve{q}^{G}_{e,t} + \sum_{s\epsilon\mathcal{S}} \breve{q}^{dc}_{s,t}\eta^{dc}_{s,t} - \sum_{s\epsilon\mathcal{S}} \breve{q}^{ch}_{s,t} = 1 \qquad t\epsilon\mathcal{T} \qquad (1j)$$

$$\sum_{g\epsilon\psi G_n} \breve{q}^{G}_{e,t} + \sum_{s\epsilon\psi S_n} \breve{q}^{dc}_{s,t}\eta^{dc}_{s,t} - \sum_{s\epsilon\psi S_n} \breve{q}^{ch}_{s,t} - \sum_{m\epsilon\Omega_n} \breve{f}_{n,m,t} = 0 \qquad n\epsilon N, t\epsilon\mathcal{T} \qquad (1k)$$

$$\hat{f}_{n,m,t} = B_{n,m}\left(\theta_{n,t} - \theta_{m,t}\right) \qquad (n,m)\epsilon\mathcal{L}, t\epsilon\mathcal{T} \qquad (1l)$$

$$\breve{f}_{n,m,t} = \phi^{T}\Delta w_t\left[B_{n,m}\left(\breve{\theta}_{n,t} - \breve{\theta}_{m,t}\right)\right] \qquad (n,m)\epsilon\mathcal{L}, t\epsilon\mathcal{T} \qquad (1m)$$

$$\theta_{n,t} = 0 \qquad n = ref, t\epsilon\mathcal{T} \qquad (1n)$$

$$\breve{\theta}_{n,t} = 0 \qquad n = ref, t\epsilon\mathcal{T} \qquad (1o)$$

The set of inequalities (1b), (1c), (1d) and (1e) are formulated as Distributionally Robust Chance Constraints (DRCCs), which aim to ensure that each constraint is met with a high level of confidence. Specifically, the optimization model accounts for the possibility of a violation of each constraint and constrains the probability of violation to be at most ϵ, or equivalent, with a confidence level of at least (1-ϵ), at the optimal solution. Therefore, the DRCCs provide a means to handle uncertainty in the optimization problem and guarantee the feasibility of the solution with a desired level of confidence.

In the inequality (1b), $\hat{q}^{G}_{g,t}$ is the quantity of power that the generator G produces at time t in day-ahead, $\breve{q}^{G}_{g,t}$ is the quantity that the generator G generates at time t in real-time which is also dependent on the Δw_t (wind deviation at time t), and $\overline{Q}^{G}_{g}$ is the maximum capacity of the generator G. To put it in general words, the power produced in the day-ahead and quantity at the real time associated with the wind deviation altogether should be less than equal than the maximum capacity of the generator. The probability that this constraint holds should be greater equal to $(1-\varepsilon)$. Supposing ε is 0.01, the constraint shows that 99% of the time the mentioned probability should hold. In the inequality (1c), the lower bound of the generator's power generation is a matter of concern and the power produced in the day-ahead and quantity at the real time should be more than equal to the minimum capacity of the generator G ($\underline{Q}^{G}_{g}$). Certain generators are constrained in their ability to operate at less than 10% of their maximum capacity. For instance, a generator with a 1000 MW capacity cannot operate below 100 MW due to technical limitations. Therefore, the generator cannot continuously operate between zero and 1000 MW but can only function within a range from 10% to its nominal value.

Regarding the inequality (1d) and (1e), $\hat{f}_{n,m,t}$ is the amount of power that flows overline connecting node "n" and "m" at time t in the deterministic fashion, $\breve{f}_{n,m,t}$ is the amount of power flow between nodes "n" and "m" at time t in the real-time and the $\overline{f}_{n,m,t}$ is the maximum amount of power flow between nodes "n" and "m" at time t. Like the previous constraints, (1d) and (1e) are both defining a high and low bound for the power flow stating that the total power flows in the day-ahead and real time between nodes "n" and "m" at time t should be between the

minimum capacity of line between these nodes at time t ($\underline{f}_{n,m,t}$) and the maximum amount ($\overline{f}_{n,m,t}$). It goes without saying that each of these constraints should hold a probability greater equal to $(1-\varepsilon)$.

In the constraint (1f), a deterministic demand assumption is adopted, except for storage, which is treated as a separate variable. Although the charging of storage can be interpreted as a form of demand, it is considered separately from absolute consumer demand. As a result, storage is modeled distinctly, and accounted for as a separate variable. It is imperative to note that this approach ensures that the treatment of storage does not interfere with the modeling of absolute consumer demand. $\underline{Q}_d^D$ and $\overline{Q}_d^D$ are the minimum and maximum amount of the demand respectively.

Respecting constraint (1g), $\tilde{q}_{d,t}^W$ is the quantity of the power generated by the wind turbine both in deterministic fashion and the uncertainty dependent. As it is obvious in the mentioned constraint it is bound between a lower band and an upper band which are the minimum and maximum wind power generation ($\underline{Q}_w^W, \overline{Q}_w^W$). When dealing with wind energy, it's important to focus on wind deviation as the initial factor. This means that any changes in wind production during the day will have a ripple effect on all other adjustments made in real-time to compensate for the mismatch. Although the committed wind amount will remain constant, other variables will be altered to balance the equation (It is modeled in a way where factors are kept constant, but the deviation that occurs is addressed by extracting it from the wind source and subtracting it from other variables.). Ultimately, the result will be $\tilde{q}_{d,t}^W$, which is essentially the same as $q_{d,t}^W$ (without the tilde symbol).

The auxiliary variable $\alpha_{g,t}$ is incorporated into the objective function to capture the cost of the real-time service provided by a generator. Its positivity is a fundamental characteristic, irrespective of whether the generator decides to increase or decrease its production. The original definition of $\alpha_{g,t}$ is manifested through the constraint (1h). It is noteworthy that $\breve{q}_{g,t}$ is a function of Δw_t, rendering it dimensionless, and is an affine function of uncertainty. Thus, $\breve{q}_{g,t}$ is not expressed in power units but represents the quantity of interest in the power system. To determine the actual amount of MW or KW supplied, $\breve{q}_{g,t}$ is multiplied by Δw_t, which converts the dimensionless variable to the appropriate physical units.

The purpose of constraint (1i) is to establish the power balance within the power system. The power balance constraint is a fundamental equation in power systems that represents the principle of conservation of energy (Grainger & Stevenson, 1994). It ensures that the total power flowing into a network must always equal the total power flowing out of the network, considering all power sources, loads, and losses within the network. Mathematically, the power balance constraint is expressed as an equality equation that equates the total power injection to the total power demand at each node or bus in the network. This constraint is critical for maintaining system stability, reliability, and safety in the face of constantly changing system conditions and operating scenarios (Kundur, 1994).

The equation 3i delineates the energy flow in a power system, with the left-hand side representing the set of energy producers and the right-hand side representing the set of energy

consumers. $\sum_{g\epsilon\psi G_n} \hat{q}^G_{e,t}$ indicates all the power produced by the generator G at time t, $\sum_{w\epsilon\psi W_n} \hat{q}^W_{w,t}$ is all the wind generation by the wind turbines at time t, $\sum_{s\epsilon\psi S_n} \hat{q}^{dc}_{s,t}\, \eta^{dc}_{s,t}$ is the generation due to the discharge of the storage s at time t, $\sum_{d\epsilon\psi D_n} \hat{q}^D_{d,t}$ shows the total demand of the consumers at time t, $\sum_{s\epsilon\psi S_n} \hat{q}^{ch}_{s,t}$ is the amount of energy consumed by the storage s at time t while charging and $\sum_{m\epsilon\Omega_n} \hat{q}_{n,m,t}$ is the amount of energy that is exported to other nodes. It should be noted that $\eta^{dc}_{s,t}$ is the efficiency of discharging.

The constraints (1j) and (1k) are dedicated to the stochastic part pf the power balance constraints. In constraint 1j, $\sum_{g\epsilon G} \breve{q}^G_{e,t}$ shows the total normalized energy produced by the conventional generators at time t, $\sum_{s\epsilon\mathcal{S}} \breve{q}^{dc}_{s,t}\eta^{dc}_{s,t}$ is the total energy generated by the storage s at time t while discharging in stochastic fashion and $\sum_{s\epsilon\mathcal{S}} \breve{q}^{ch}_{s,t}$ is the total stochastic energy consumption of the storage s at time t. It is important to know that every element in this equation is normalized by the wind deviation and 1 represents the total wind deviation per time t. To put it in another words if the equation is multiplied in $\phi^T \Delta w_t$, the right side of the equation would equal to total wind deviation and the left side will show the absolute value (MW). It is prudent to mention that all the demand is considered to be deterministic and that's the reason it has been omitted from the stochastic power balance constraints.

Constraint (1l) and (1m) demonstrate the simplest way of modeling the power flows between the nodes in a power system in a deterministic fashion and real-time, respectively. As mentioned earlier, $\hat{f}_{n,m,t}$ is the amount of power that flows overline connecting node "n" and "m" at time t in the deterministic fashion. In the constraints (1n) and (1o), $\theta_{n,t} = 0$ and $\breve{\theta}_{n,t} = 0$ the node n at time t is considered to be the reference node (slack bus) both in deterministic fashion and real-time and that is the reason it is considered to be equal to zero. In power systems, the term "slack bus" or "slack generator" refers to a bus or generator that is designated as the reference point for the calculation of system voltages and power flows. The slack bus is used to balance the power flow in the system by adjusting its output to ensure that the total power generated in the system equals the total power consumed (Stagg & El Abiad, n.d.). The slack bus is also known as the reference bus or reference generator, and it is usually chosen to be the bus or generator with the highest voltage in the system (Wood et al., 2013). By setting the voltage magnitude and phase angle at the slack bus, the voltage at all other buses in the system can be calculated using the power flow equations. This allows for the determination of power flows and system stability analysis.

The angle of the voltage at the slack bus is typically set to zero in power system calculations because the slack bus serves as the reference point for phase angles in the system. When analyzing a power system, it is necessary to calculate the phase angle differences between different buses in the system in order to determine the power flows and voltages at each bus. By designating the voltage angle at the slack bus as zero, the phase angles at all other buses in the system can be calculated relative to the slack bus angle (Kundur, 1994). Setting the slack bus angle to zero simplifies the calculation of power flows and voltages in the system and eliminates the need to explicitly calculate the phase angles at the slack bus. Additionally, since the slack bus is typically chosen to be the bus with the highest voltage in the system, setting its

angle to zero allows for a consistent reference point for phase angle calculations across the entire power system (Grainger & Stevenson, 1994).

2.2.2.2 Storage Constraints

In this section, the limitations related to storage capacity are introduced and discussed. It should be noted that there are different views to tackle the problem that this thesis is trying to solve which will be explained later in the Appendix A. The following storge constraints are derived from method 3.

$$0 \leq e_{s,t} \leq \overline{E}_s \qquad s\epsilon\mathcal{S}, t\epsilon\mathcal{T} \qquad (2a)$$

$$\hat{e}_{s,t} = \hat{e}_{s,t-1} + \hat{q}^{ch}_{s,t}\eta^{ch}_s - \hat{q}^{dc}_{s,t}: \qquad \left(\lambda^e_{s,t}\right) \qquad s\epsilon\mathcal{S}, t\epsilon\mathcal{T} \qquad (2b)$$

$$\check{e}_{s,t} = \check{e}_{s,t-1} + \check{q}^{ch}_{s,t}\eta^{ch}_s - \check{q}^{dc}_{s,t}: \qquad \left(\lambda^e_{s,t}\right) \qquad s\epsilon\mathcal{S}, t\epsilon\mathcal{T} \qquad (2c)$$

$$\underset{\mathbb{P}\epsilon\mathrm{II}}{\mathrm{Min}}\mathbb{P}\left[\hat{e}_{s,t} + (\phi^T\Delta w_t)\check{q}^{ch}_{s,t}\eta^{ch}_s \leq \overline{E}_s\right] \geq (1-\varepsilon) \qquad s\epsilon\mathcal{S}, t\epsilon\mathcal{T} \qquad (2d)$$

$$\underset{\mathbb{P}\epsilon\mathrm{II}}{\mathrm{Min}}\mathbb{P}\left[(\phi^T\Delta w_t)\check{q}^{dc}_{s,t} \leq \hat{e}_{s,t}\right] \geq (1-\varepsilon) \qquad s\epsilon\mathcal{S}, t\epsilon\mathcal{T} \qquad (2e)$$

$$0 \leq \hat{q}^{ch}_{s,t} \leq \overline{\hat{Q}^{ch}_{s,t}} \qquad s\epsilon\mathcal{S}, t\epsilon\mathcal{T} \qquad (2f)$$

$$0 \leq \hat{q}^{dc}_{s,t} \leq \overline{\hat{Q}^{dc}_{s,t}} \qquad s\epsilon\mathcal{S}, t\epsilon\mathcal{T} \qquad (2g)$$

$$\underset{\mathbb{P}\epsilon\mathrm{II}}{\mathrm{Min}}\mathbb{P}\left[\hat{q}^{ch}_{s,t} + (\phi^T\Delta w_t)\check{q}^{ch}_{s,t} - \hat{q}^{dc}_{s,t} \leq \overline{Q_s}\right] \geq (1-\varepsilon) \qquad s\epsilon\mathcal{S}, t\epsilon\mathcal{T} \qquad (2h)$$

$$\underset{\mathbb{P}\epsilon\mathrm{II}}{\mathrm{Min}}\mathbb{P}\left[\hat{q}^{dc}_{s,t} + (\phi^T\Delta w_t)\check{q}^{dc}_{s,t} - \hat{q}^{ch}_{s,t} \leq \overline{Q_s}\right] \geq (1-\varepsilon) \qquad s\epsilon\mathcal{S}, t\epsilon\mathcal{T} \qquad (2i)$$

$$\check{q}_{s,t} = \check{q}^{dc}_{s,t} - \check{q}^{ch}_{s,t} \qquad s\epsilon\mathcal{S}, t\epsilon\mathcal{T} \qquad (2j)$$

$$\sum_{t\epsilon\mathcal{T}}\left[p^{sprd}_s\hat{q}^{ch}_{s,t} + C^{Av}_s\beta_{s,t}\right] \geq I^0_s + I^E_s\overline{E}_s + I^Q_s\overline{Q}_s \qquad s\epsilon\mathcal{S}, t\epsilon\mathcal{T} \qquad (2k)$$

$$\beta_{s,t} \leq (\phi^T\Delta w_t)\check{q}_{s,t} \qquad s\epsilon\mathcal{S}, t\epsilon\mathcal{T} \qquad (2l)$$

$$p_s spread \geq 0 \qquad s\epsilon\mathcal{S} \qquad (2m)$$

$$\overline{E}_s \geq 0 \qquad s\epsilon\mathcal{S} \qquad (2n)$$

$$\overline{Q}_s \geq 0 \qquad s\epsilon\mathcal{S} \qquad (2o)$$

Constraints (2a), (2b) and (2c) are dedicated to defining the energy state of the storage in the deterministic and rea-time. $e_{s,t}$ shows the overall energy state of storage s at time t, while $\hat{e}_{s,t}$ and $\check{e}_{s,t}$ indicate the energy state of the storage s at time t in a deterministic fashion and real time respectively. Accordingly, $\hat{e}_{s,t-1}$ and $\check{e}_{s,t-1}$ are the energy state of the storage s, in day-ahead and real time at time t-1. As described before $\hat{q}^{ch}_{s,t}$ is the quantity of the energy charged by the

storage s at time t in day-ahead, $\hat{q}_{s,t}^{dc}$ is the quantity of the energy discharged by the storage s at time t, $\check{q}_{s,t}^{ch}$ show the quantity of the energy charged by the storage s at time t and $\check{q}_{s,t}^{dc}$ indicates the amount of discharged energy by the storage s at time t in real-time. It should be noted that the η_s^{ch} is the efficiency of charging of the storage s, which is assumed to be 0.95. The mentioned constraints define the storage state in day-ahead and real-time. The amount of energy stored in the storage equals to the amount of energy which was stored in the storage by the end of the last operating state plus the amount of energy that is being charged in it and discharged from it. Constraint (2a) also indicates that the amount of energy stored in the storage at time t, cannot exceed the maximum amount of the storage state ($\overline{E}_s$). It is also prudent to mention that at time t=1, the term $\hat{e}_{s,t-1}$ and $\check{e}_{s,t-1}$ are defined as the initial state of the storage in the day-ahead and real-time respectively.

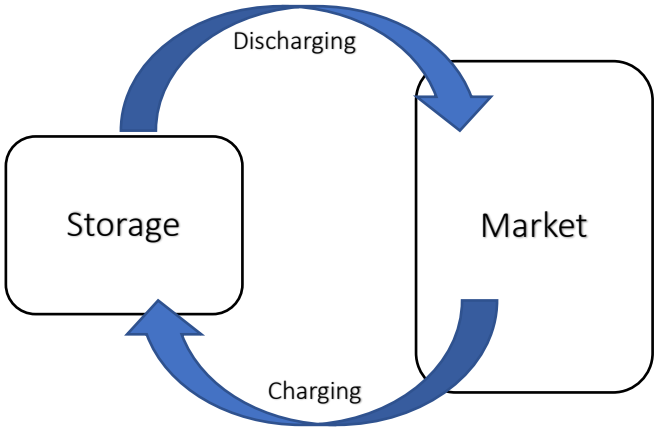

Figure 1- energy transition between market and the storage

As shown in figure 1, $q_{s,t}^{ch}$ is defined when the energy leaves the market and $q_{s,t}^{dc}$ shows the amount of energy leaving the storage. What should be noted is the fact that if $q_{s,t}^{dc}$ is leaving the storage, the actual amount of energy entering the market is $q_{s,t}^{dc}\eta_s^{dc}$. Although since storage is the matter of concern here all the energy transition from and to the storage is considered for defining the constraints.

The Distributionally Robust Chance Constraints (DRCCs) consist of a group of inequalities (2d), (2e), (2h), and (2i) in the storage, which are designed to ensure that each constraint is fulfilled with a high level of assurance. The DRCCs are formulated in such a way that the optimization model takes into account the possibility of violating each constraint and restricts the probability of violation to no more than ϵ. This is equivalent to achieving a confidence level of at least (1-ϵ) at the optimal solution. Consequently, the DRCCs offer a way to deal with uncertainty in the optimization problem and guarantee the feasibility of the solution with a desired level of confidence.

Constraint (2d) indicates that the sum of storage state at time t in day-ahead and the quantity of energy charged in the storage in real-time should not exceed the maximum energy capacity of the storage. To satisfy the constraint, it is necessary that the probability of it being true is no less than (1-ε). For example, if ε is equal to 0.01, the constraint indicates that the probability should be met at least 99% of the time. It should be noted that since both the real-time and day-ahead variables are used in a constraint, $\phi^T \Delta w_t$ has been used to normalize all the variables. Constraint (2d) states that the quantity of electricity discharged from the storage s at time should be less than the energy state of the storage s at time t in day-ahead. It is also prudent to mention that the reason for considering the constraints as displayed will be fully explained later in Appendix A.

Constraints (2f) and (2g) are defining lower and higher bound for the quantity of charging and discharging of the storage s at time t in a deterministic fashion. Each of the charging and discharging quantity should be lower than the maximum quantity of charging of storage s at time t in day ahead and maximum amount of energy discharged from the storage s at time t, respectively.

As mentioned before, constraints (2h) and (2g) are also formulated as DRCC in which the goal is to ensure that each of the constraints is met with high level of confidence. The reason that these constraints are formulated as the way they are shown will be fully covered in appendix A. Constraint (2h) states that sum of the real-time quantity of charging of the storage s at time t ($\breve{q}_{s,t}^{ch}$) and the quantity of charging in the storage s at time t ($\hat{q}_{s,t}^{ch}$) and discharging ($\hat{q}_{s,t}^{dc}$) must not exceed from the maximum rating capacity of the storage ($\overline{Q_s}$). Constraint (2i) indicates that the real-time quantity of discharge in storage s at time t ($\breve{q}_{s,t}^{dc}$), plus the day-ahead amount of the energy discharged from the storage ($\hat{q}_{s,t}^{dc}$) minus the day-ahead quantity of energy charged in the storage ($\hat{q}_{s,t}^{ch}$) should be less than equal to the maximum power rating capacity as well. The probability that these two constraints hold should be greater equal to $(1-\varepsilon)$. Supposing ε is 0.01, the constraints show that 99% of the time the mentioned probability should hold.

As the constraint (2j) demonstrates, the total quantity of storage power in real-time ($\breve{q}_{s,t}$) equals the difference between the quantity of power discharging from storage s in real time and the real-time amount of power charging in the storage s at time t.

$p_s^{sprd} \hat{q}_{s,t}^{ch}$ in the constraint (2k) indicates how much money is made based on price spread times the amount of power you charge (how much profit has been made by the market arbitrage), while $C_s^{Av} \beta_{s,t}$ indicates how much the storage has made by providing charging and discharging services. This constraint states that the sum of all the benefits made by storage and the market arbitrage should exceed the investment cost of the storage. Market arbitrage is a well-known practice in finance, often used to exploit price discrepancies in financial markets. According to (Hull et al., n.d.), market arbitrage is the process of taking advantage of price differences for the same asset or security in different markets. By buying the asset or security in one market where the price is lower and selling it in another market where the price is higher, arbitrageurs can earn a profit from the price difference. This process of arbitrage is crucial in keeping the prices of the same asset or security in different markets in line with each other

(Shiller, 2015). One assumption here is that storage is a linear function of the maximum energy capacity ($\overline{E}_s$) and the maximum power rating capacity ($\overline{Q}_s$). It should be noted that I_s^0 is the base cost of storage implementation and in case of this thesis, it is assumed that there is only one location that one storage is going to be built in. $\beta_{s,t}$ is the flexibility of charging and discharging of the storage s.

Regarding the constraints (2m), (2n) and (2o), the lower bounds of the price difference, the maximum energy capacity ($\overline{E}_s$) and the maximum power rating capacity ($\overline{Q}_s$) has been defined. As is noticeable from the constraints, these are all non-negative.

2.2.3 SOC reformulation of probabilistic problem

DRCC is a well-established concept in decision-making under uncertainty. It is widely used in fields such as finance, operations research, and engineering (Bental et al., 2015; Hong et al., 2019). When formulating a DRCC, the decision maker seeks to optimize a certain objective while satisfying a constraint that must hold with a certain probability, regardless of the underlying probability distribution. This approach is useful when the decision maker has limited information about the underlying probability distribution or when the distribution is uncertain or ambiguous (Shapiro et al., 2014).

However, DRCC constraints cannot be numerically solved by the optimization model and require reformulation. One approach is to use an ambiguity set that includes all distributions with the same first and second moments (Bental et al., 2015). The minimum is then selected as a solution. It is important to note that the constraint is non-linear and infinite-dimensional in both cases. To resolve this, Shebyshev's findings can be used to demonstrate that DRCC constraints are equivalent to a second-order cone constraint (Hong et al., 2019).

Regarding what has been stated in the previous paragraphs, it can be said that $(\phi^T \Delta w_t)\breve{q} \coloneqq \breve{q}\mu(\breve{q}) + \sqrt{\frac{1-\epsilon}{\epsilon}}\left\|\breve{q}\Sigma^{1/2}\right\|^2$, which for the sake of brevity can be written as $\acute{\varepsilon}.\gamma_t.\breve{q}$, where $\acute{\varepsilon} \coloneqq \sqrt{\frac{1-\epsilon}{\epsilon}}$ and $\breve{q}\gamma_t \coloneqq \left\|\breve{q}\Sigma^{1/2}\right\|^2$. Assuming an affine response policy to account for uncertainty and a zero mean forecast error, the objective function problem and the power and storage constraints can be represented as follows:

$$\underset{\Xi,\mathbb{P}\epsilon\Pi}{\text{Min}} \sum_{t\epsilon\mathcal{T}} \left[\left(\sum_{g\epsilon\mathcal{G}} \breve{q}_{g,t}^{G} p_{g,t}^{G} - \sum_{d\epsilon\mathcal{D}} q_d^D p_{d,t}^D + \sum_{s\epsilon\mathcal{S}} p_s^{sprd} \breve{q}_{s,t}^{ch} \right) + \sum_{g\epsilon\mathcal{G}} C_g^{Av} \alpha_{g,t} + \sum_{s\epsilon\mathcal{S}} C_s^{Av} \beta_{s,t} \right] \quad (3a)$$

The primary idea conveyed is that the proposed method provides a numerical representation of DRCC constraints in the form of Second Order Cone (SOC) problems. In the subsequent sections of this segment, the reformulated power and storage constraints will be represented.

2.2.3.1 Power constraints

This section presents and examines the limitations related to the power system, including the constraints pertaining to generators, loads, and wind power, which have been reformulated as SOC problems.

$$\acute{\varepsilon}.\gamma_t.\breve{q}^G_{g,t} \le \overline{Q}^G_g - \hat{q}^G_{g,t} \qquad g\epsilon G, t\epsilon\mathcal{T} \qquad (3b)$$

$$\acute{\varepsilon}.\gamma_t.\breve{q}^G_{g,t} \ge \underline{Q}^G_g - \hat{q}^G_{g,t} \qquad g\epsilon G, t\epsilon\mathcal{T} \qquad (3c)$$

$$\acute{\varepsilon}.\gamma_t.\breve{f}_{n,m,t} \le \overline{f}_{n,m,t} - \hat{f}_{n,m,t} \qquad (n,m)\epsilon\mathcal{E}_n, t\epsilon\mathcal{T} \qquad (3d)$$

$$\acute{\varepsilon}.\gamma_t.\breve{f}_{n,m,t} \ge \underline{f}_{n,m,t} - \hat{f}_{n,m,t} \qquad (n,m)\epsilon\mathcal{E}_n, t\epsilon\mathcal{T} \qquad (3e)$$

$$\underline{Q}^D_d \le q^D_{d,t} \le \overline{Q}^D_d \qquad d\epsilon\mathcal{D} \qquad (3f)$$

$$\underline{Q}^W_w \le \tilde{q}^W_{d,t} \le \overline{Q}^W_w \qquad w\epsilon W \qquad (3g)$$

$$\alpha_{g,t} \ge \acute{\varepsilon}.\gamma_t.\breve{q}_{g,t} \qquad g\epsilon G, t\epsilon\mathcal{T} \qquad (3h)$$

$$\sum_{g\epsilon\psi G_n} \hat{q}^G_{e,t} + \sum_{w\epsilon\psi W_n} \hat{q}^W_{w,t} + \sum_{s\epsilon\psi S_n} \hat{q}^{dc}_{s,t}\,\eta^{dc}_{s,t} = \sum_{d\epsilon\psi D_n} \hat{q}^D_{d,t} + \sum_{s\epsilon\psi S_n} \hat{q}^{ch}_{s,t} + \sum_{m\epsilon\Omega_n} \hat{q}_{n,m,t} \qquad n\epsilon N, t\epsilon\mathcal{T} \qquad (3i)$$

$$\sum_{g\epsilon G} \breve{q}^G_{e,t} + \sum_{s\epsilon\delta} \breve{q}^{dc}_{s,t}\eta^{dc}_{s,t} - \sum_{s\epsilon\delta} \breve{q}^{ch}_{s,t} = 1 \qquad t\epsilon\mathcal{T} \qquad (3j)$$

$$\sum_{g\epsilon\psi G_n} \breve{q}^G_{e,t} + \sum_{s\epsilon\psi S_n} \breve{q}^{dc}_{s,t}\eta^{dc}_{s,t} - \sum_{s\epsilon\psi S_n} \breve{q}^{ch}_{s,t} - \sum_{m\epsilon\Omega_n} \breve{f}_{n,m,t} = 0 \qquad n\epsilon N, t\epsilon\mathcal{T} \qquad (3k)$$

$$\hat{f}_{n,m,t} = B_{n,m}\left(\theta_{n,t} - \theta_{m,t}\right) \qquad (n,m)\epsilon\mathcal{L}, t\epsilon\mathcal{T} \qquad (3l)$$

$$\breve{f}_{n,m,t} = \phi^T \Delta w_t\left[B_{n,m}\left(\breve{\theta}_{n,t} - \breve{\theta}_{m,t}\right)\right] \qquad (n,m)\epsilon\mathcal{L}, t\epsilon\mathcal{T} \qquad (3m)$$

$$\theta_{n,t} = 0 \qquad n = ref, t\epsilon\mathcal{T} \qquad (3n)$$

$$\breve{\theta}_{n,t} = 0 \qquad n = ref, t\epsilon\mathcal{T} \qquad (3o)$$

As previously mentioned, the inequalities (1b), (1c), (1d), and (1e) are expressed as DRCCs to ensure a high level of confidence in satisfying each constraint (these constraints have changed to (3b), (3c), (3d) and (3e)). Other constraints, which remain unchanged after relaxation, will not be further discussed. Constraints (3b) and (3c) are defining a lower and upper bound for the amount of power generation in real-time by generator g at time t, and the constraints (3d) and (3e) are presenting the bounds for the amount of power that flows overline connecting node n to node m in real-time at time t.

2.2.3.2 Storage constraints

This section presents and discusses the constraints related to storage capacity, which have been modified as a result of the SOC relaxation.

$$0 \leq e_{s,t} \leq \overline{E}_s \qquad s\epsilon\mathcal{S}, t\epsilon\mathcal{T} \qquad (4a)$$

$$\hat{e}_{s,t} = \hat{e}_{s,t-1} + \hat{q}^{ch}_{s,t}\eta^{ch}_s - \hat{q}^{dc}_{s,t}: \qquad \left(\lambda^e_{s,t}\right) \qquad s\epsilon\mathcal{S}, t\epsilon\mathcal{T} \qquad (4b)$$

$$\check{e}_{s,t} = \check{e}_{s,t-1} + \check{q}^{ch}_{s,t}\eta^{ch}_s - \check{q}^{dc}_{s,t}: \qquad \left(\lambda^e_{s,t}\right) \qquad s\epsilon\mathcal{S}, t\epsilon\mathcal{T} \qquad (4c)$$

$$0 \leq \acute{\varepsilon}.\gamma_t.\check{q}^{ch}_{s,t}\eta^{ch}_s \leq \overline{E}_s - \hat{e}_{s,t} \qquad s\epsilon\mathcal{S}, t\epsilon\mathcal{T} \qquad (4d)$$

$$0 \leq \acute{\varepsilon}.\gamma_t.\check{q}^{dc}_{s,t} \leq \hat{e}_{s,t} \qquad s\epsilon\mathcal{S}, t\epsilon\mathcal{T} \qquad (4e)$$

$$0 \leq \hat{q}^{ch}_{s,t} \leq \overline{\hat{Q}^{ch}_{s,t}} \qquad s\epsilon\mathcal{S}, t\epsilon\mathcal{T} \qquad (4f)$$

$$0 \leq \hat{q}^{dc}_{s,t} \leq \overline{\hat{Q}^{dc}_{s,t}} \qquad s\epsilon\mathcal{S}, t\epsilon\mathcal{T} \qquad (4g)$$

$$0 \leq \acute{\varepsilon}.\gamma_t.\check{q}^{ch}_{s,t} \leq \left(\overline{Q_s} - \hat{q}^{ch}_{s,t}\right) + \hat{q}^{dc}_{s,t} \qquad s\epsilon\mathcal{S}, t\epsilon\mathcal{T} \qquad (4h)$$

$$0 \leq \acute{\varepsilon}.\gamma_t.\check{q}^{dc}_{s,t} \leq \left(\overline{Q_s} - \hat{q}^{dc}_{s,t}\right) + \hat{q}^{ch}_{s,t} \qquad s\epsilon\mathcal{S}, t\epsilon\mathcal{T} \qquad (4i)$$

$$\check{q}_{s,t} = \check{q}^{dc}_{s,t} - \check{q}^{ch}_{s,t} \qquad s\epsilon\mathcal{S}, t\epsilon\mathcal{T} \qquad (4j)$$

$$\sum_{t\epsilon\mathcal{T}}\left[p^{sprd}_s\hat{q}^{ch}_{s,t} + C^{Av}_s\beta_{s,t}\right] \geq I^0_s + I^E_s\overline{E}_s + I^Q_s\overline{Q}_s \qquad s\epsilon\mathcal{S}, t\epsilon\mathcal{T} \qquad (4k)$$

$$\beta_{s,t} \geq \acute{\varepsilon}.\gamma_t.\check{q}_{s,t} \qquad s\epsilon\mathcal{S}, t\epsilon\mathcal{T} \qquad (4l)$$

$$p_s spread \geq 0 \qquad s\epsilon\mathcal{S} \qquad (4m)$$

$$0 \leq \overline{E}_s \leq U_s M \qquad s\epsilon\mathcal{S} \qquad (4n)$$

$$0 \leq \overline{Q}_s \leq U_s M \qquad s\epsilon\mathcal{S} \qquad (4o)$$

As mentioned before, constraints (2d), (2e), (2h) and 2i are designed to ensure that each constraint is fulfilled with a high level of assurance, but as stated before in order to have the DRCC constraints numerically solved by the optimization model, these constraints must be reformulated as SOC problems. Constraint (4d) indicates a lower and upper bound for the amount of power charged by the storage s at time t in real-time. Constraint (4e) states that the amount pf power discharged from the storage s at time t in real time should not exceed the energy state storage at time t which means that the storage cannot discharge more that amount of energy it is containing at time t. Not only should this limitation be examined by the maximum of the storage state but also the maximum capacity of the storage ($\overline{Q_s}$) must be taken into account as well. Constraints (4h) and (4i) try to focus on the mentioned limitation while the storage is in charging and discharging state. Appendix A will give a clearer perspective on these constraints.

3 Results and Discussion

This study aimed to investigate the strategic market participation of an energy storage system in a competitive electricity market, considering short-run uncertainties. The central research question guiding this study was to explore the feasibility of developing a robust method for modeling a power grid with storage capacity that considers the various distribution possibilities in an uncertain environment.

Electricity storage systems have become essential to the modern power system (Denholm et al., 2010). They provide flexibility in managing the variability and uncertainty of renewable energy sources, enhance grid reliability and security, and reduce greenhouse gas emissions (Katiraei et al., 2008). With the increasing penetration of renewable energy sources, energy storage systems are becoming increasingly essential to ensure grid stability and support the integration of intermittent renewable energy (Energy Agency, 2020). In this context, energy storage systems must participate in electricity markets and generate revenue streams.

However, the participation of energy storage systems in electricity markets is challenging, particularly in a competitive environment, due to short-run uncertainties, such as fluctuating electricity prices, demand variability, and uncertain renewable energy generation (Weron, 2014). These uncertainties can lead to suboptimal decisions and revenue losses for energy storage systems, resulting in reduced profitability and operational inefficiencies.

To address these challenges, a robust modeling approach that accounts for short-run uncertainties is required to enable energy storage systems to participate in electricity markets efficiently. In this study, we proposed a novel method to model the strategic market participation of an energy storage system in a competitive electricity market, considering short-run uncertainties. The proposed method incorporates a stochastic optimization approach that optimizes the storage system's operation in response to market prices, demand, and renewable energy generation (X. Luo et al., 2018). We applied the proposed method to a case study of a hypothetical power grid with storage capacity and evaluated its performance under different short-run uncertainties.

The results of this study demonstrate the feasibility and effectiveness of the proposed method for modeling energy storage systems' market participation in a competitive electricity market, considering short-run uncertainties. The proposed method enable energy storage systems to maximize their revenue streams while contributing to grid stability and enhancing the integration of renewable energy sources (Pourmousavi et al., 2015).

In this section, a baseline case study will be defined, and based on the results obtained from the baseline case, all the figures and their explanations will be reviewed. Then, a sensitivity analysis will be performed under three scenarios to perceive the adequate practicals of the problem formulations. This will lead into the next section of the thesis report, conclusion, and result, where research questions will be answered.

3.1 Case study

To tackle the main research question of this thesis, the investigated power network will consist of 12 conventional generators, two wind farms with a maximum capacity of 500 MW each, 17 conventional loads, and a hypothetical storage with a charging and discharging efficiency of 95 percent. The violation probability ϵ is fixed at 0.1 for all the DRCCs. In the baseline case, the availability costs for conventional generators C_g^{Av} and the availability cost for the storage both in the charging and discharging C_s^{Av} are set to an initial value of 100 €/MW and 10 €/MW respectively. All the investment costs related to the storage are set to a fixed number and will be discussed thoroughly in the sensitivity analysis section. The term "availability cost" refers to the cost incurred by flexible assets to provide the flexibility service (Chio et al., 2019). This includes maintenance and operational costs required to ensure the assets are available when needed (Wang et al., 2018). In other words, it represents the monetary expenditure necessary to maintain the readiness of the assets to offer the required flexibility services (X. J. Luo et al., 2020).

Julia programming language is used to solve the aforementioned objective function, which was stated in the problem formulation. Julia is a high-performance programming language designed for numerical and scientific computing, data science, and artificial intelligence applications (Bezanson et al., 2017). It combines the ease of use and syntax of Python with the speed and efficiency of lower-level languages like C and Fortran. Julia is fast due to its just-in-time (JIT) compiler that translates Julia's code into highly optimized machine code. Its simplicity and consistency make it accessible to developers with different backgrounds (Edelman et al., 2019).

Furthermore, Julia has powerful built-in features for distributed computing, which can significantly speed up optimization problems (Boyd et al., 2011), and a comprehensive ecosystem of packages, including several optimization packages such as JuMP, Convex.jl, and Optim.jl, which make it easy to implement and solve complex optimization problems (Dunning et al., 2015, 2017). The problem is implemented in Julia v1.8.5, modeled with JuMP v1.8.0, and solved with Mosek v10.0.36. It should be noted that the problem is solved with an average CPU time of 2.67 seconds using a laptop with 32GB RAM with a Processor Intel(R) Core (TM) i7-7500U CPU at 2.90 GHz.

3.2 Numerical Results

In this section, we will take a look at the result under a particular situation, go through the results one by one and have a clear understanding of the plots and what they reflect later on, in the sensitivity analysis section, by changing different factors of the problem we try to have an apprehension with a more extensive scope on the involved elements of the problem. As mentioned in section 2, there are different methods to tackle the issue in the thesis, which has been explained in appendix A, from which we have selected method number 3 to go within this

thesis. Considering different paths to solve the objective function, it is also prudent to mention that the final results are expected to be the same.

As explained earlier, to better understand the results, we will start by defining a baseline case in which we will set some of the effective indicators and go through the outcomes. Regarding the baseline, the violation probability chosen is $\epsilon = 0.1$. The availability cost of the generators (C_g^{Av}) is 100€/MW and for the storage (C_s^{Av}) is 10€/MW, which will make the participation of the storage more likely, especially with the generators cost being higher. More precisely, regarding the set values and how the availability costs of the storage are less than the generators, it is more likely for the storage to participate in the power network (charging and discharging depending on the energy prices).

Regarding the investment costs, the initial investment cost of implementing the storage (I_s^0), the storage investment cost (I_s^E), and the investment costs regarding the maximum capacity of the storage (I_s^Q) are all set to a fixed number of 2€/MW, which will guarantee the participation storage. The higher value would make the storage participation stop because of the storage constraint (4k) by making right side of the inequality very big in a way that it takes a lot of participation for the constraint to hold that somehow the mentioned condition will make it impossible. The value U_s which is binary variable is set to one. Setting the value to zero indicates that the maximum storage state ($\overline{E}_s$) and maximum capacity of the storage ($\overline{Q}_s$) must be equal to zero which shows that it is impossible to have storage in the network (constraints 4n and 4o). The value of M, which is a very big number, is also set to 1000.

Lastly, the price difference is set to a very small number like one to assure storage participation in the power network. If the price difference between energy storage charging and discharging is lower, it is likely to encourage greater participation in storage during these time periods. This is because with a lower price difference, the potential profits from using storage to charge during low price periods and discharge during high price periods become more attractive to energy storage providers. As a result, they may increase their participation in both the day-ahead and real-time markets to take advantage of these profit opportunities. The

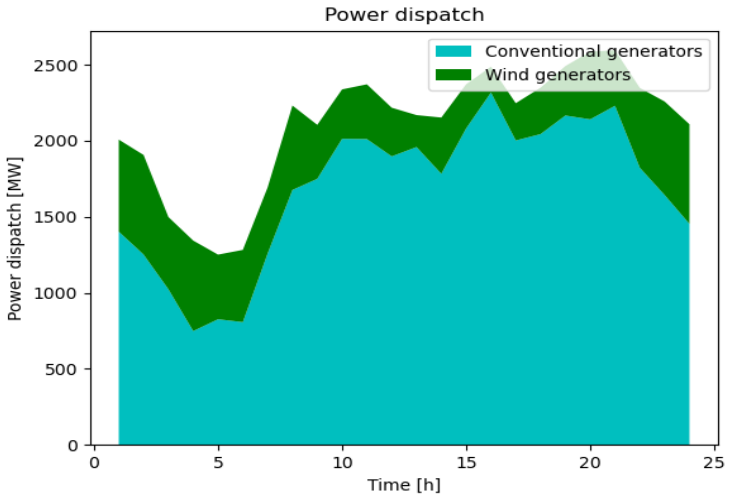

Figure 2- Scheduled DA Power dispatch.

remaining part of this section will be devoted to the results of the written objective function and code after being run for the baseline case.

The figure presented as Figure 2 demonstrates the optimal schedule for day-ahead dispatch resulting from the coordinated operation of power networks and wind generators for the baseline scenario. This scenario assumes a selected violation probability of ϵ = 0.1 and availability costs of $C_g^{Av} = 100€/MW$ for generators and $C_s^{Av} = 10€/MW$ for storage. The conventional power load, which refers to the load not associated with wind turbines, is displayed in blue in the figure. On the other hand, the power dispatch produced by the wind turbines is indicated in green. The figure highlights that the conventional generators supply the largest share of the total load, whereas the wind turbines supply the remaining portion. It is worth noting that both the conventional load and the load generated by the wind turbines fluctuate throughout the day, although the variation in the load generated by wind turbines is less than that produced by conventional generators.

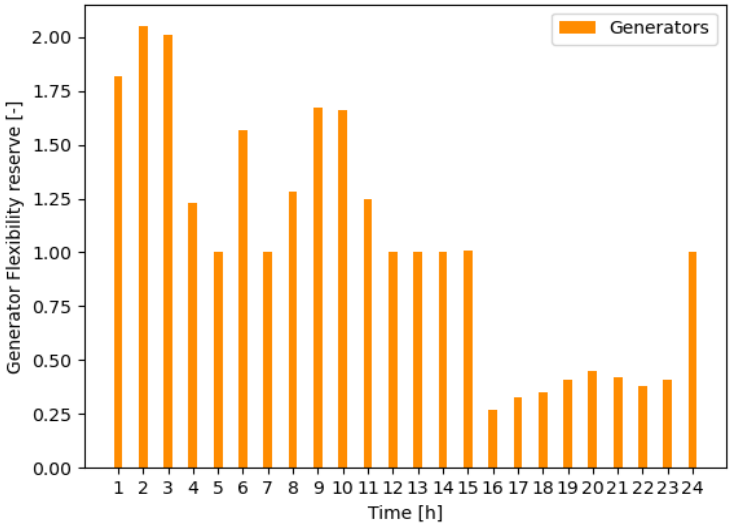

Figure 3 - Generator Flexibility Reserve.

Flexible generators are given affine policies, along with extra storage, to account for any variations in wind power during the real-time stage. These policies are designed to ensure that there is enough flexibility available to maintain a stable operation of the system during real-time operation. Figure 2 shows the provision of flexibility reserves by flexible generators. It is prudent to mention that the flexibility reserves are expressed by the unit of wind power deviation.

Like figure 3, Figure 4 also indicates the flexibility reserve assigned to the storage per Unit of wind power forecast deviation. What is important about figure 3 and 4 is that the bars indicate the amount of flexibility provided by different assets based on the description given in each figure. As illustrated in the figure 3, the positive generation reserve means the increasing amount of the energy production by the generator. The negative reserve, as shown in figure 4

between hours 1 to 12, implies an increased amount of energy consumption by the storage (charging state).

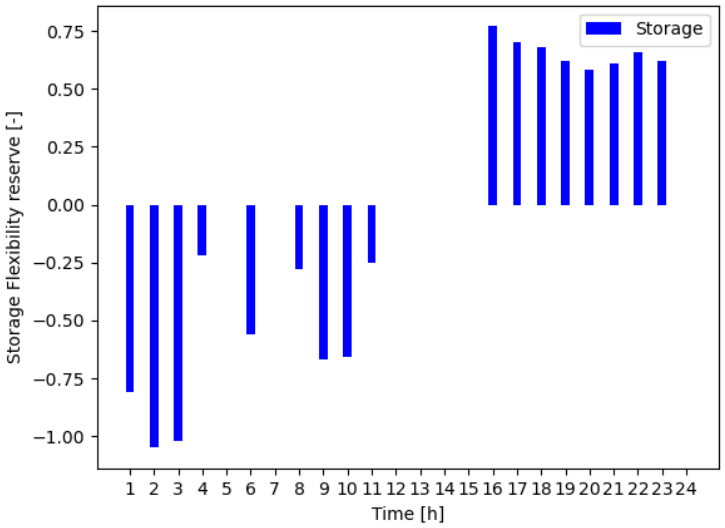

Figure 4 - Storage Flexibility Reserve.

It should be noted that the combined flexibility of generators and pumps should always equal one, indicating that any discrepancy in power supply is completely balanced out. As seen in the above figures, at certain times like hours 2, 3, 4, etc. generators may allocate extra flexibility. Despite appearing counterintuitive, this approach can aid in reducing network congestion and assigning flexibility at a minimal cost. This indicates that, depending on the location of flexible resources, network topology, and congestion levels, it may be advantageous for some flexible assets to move in the opposite direction of the system's requirements at certain times, if it leads to an improvement in the overall usefulness of the system.

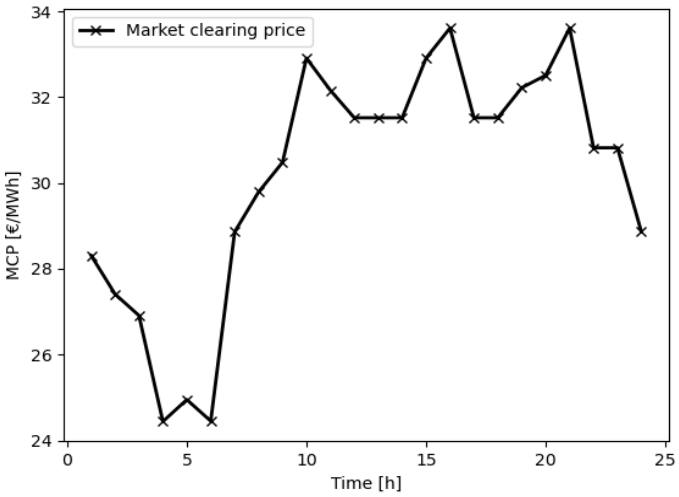

Figure 5 – Market clearing price.

When the market-clearing problem for the day-ahead market is resolved, it yields details about the market-clearing prices (MCPs), and the effect of the suggested affine policies on the overall usefulness of the system. The market clearing price is the price at which the quantity of goods or services supplied is equal to the quantity of goods or services demanded, resulting in a market equilibrium. It is determined by the intersection of the supply and demand curves in a competitive market and represents the fair value of the product or service. This price can change over time as the underlying factors affecting supply and demand (Kenton, 2022).

The market clearing price in the day-ahead (DA) market is determined by the dual variable that corresponds to the power balance constraint (3i). This dual variable is also referred to as the shadow price because it indicates the immediate impact on the objective value that would result from a one-unit change in the right-hand side of constraint (3i). As is evident in figure 5, the MCP fluctuates during the day in response to changes in both the cost of generating power and the total demand for electricity on the network. Between hours 1 and 8, the MCPs fluctuate between 24 and 30 €/MW, which is relatively lower than the MCPs between the hours 8 and 21. The reason for MCPs at the start of the day is a combination of a lower overall demand for electricity on the network and greater availability of wind power. As demand increases and wind power generation decreases, the MCPs rise. During the last few hours of the day (between hours 21 and 24), the MCPs decreased due to an increase in wind power generation.

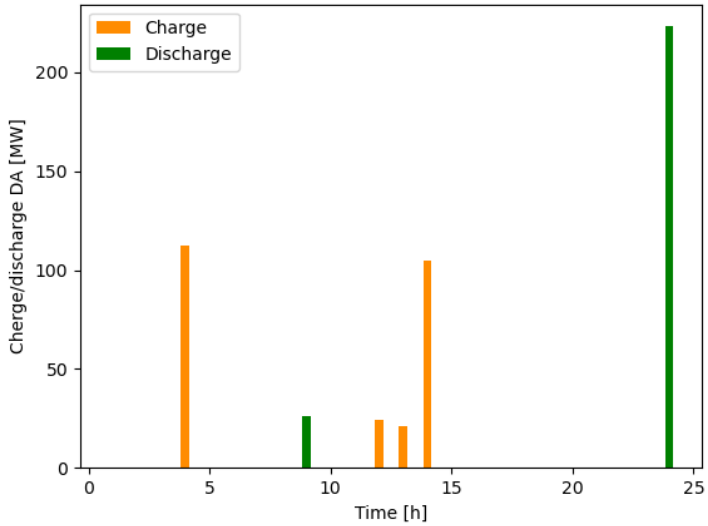

Figure 6 – Day-ahead Charging and discharging of the storage.

Figure 6 shows the charging and discharging of the storage in the day-ahead (DA) market. The orange bars are the representatives of the times that storage undergoes charging state while the green bars indicate the discharging of the storage. By looking at the figure and also considering the market clearing price figure (figure 4), it can be understood that the charging is at its peak while the MCP is at its lowest or experiencing a relative decrease like in hours 4 or between hours 12 to 14, respectively.

As mentioned in previous sections, the day-ahead and real-time market are both important components of the electricity market; therefore, to have a better understanding of the battery participation and have clearer interpretation, another figure should be taken into account which implies charging and discharging of the storage in the real-time.

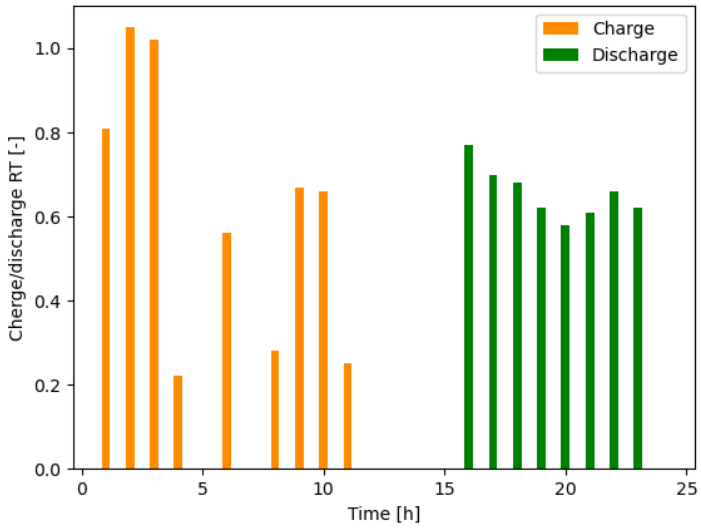

Figure 7 – Real-time Charging and discharging of the storage.

Figure 7 indicates the charging and discharging of the storage in the real-time (RT) market. Similar to figure 6, the orange bars represent the time intervals during which energy storage is being charged, while the green bars indicate the time intervals during which the storage is being discharged. It should be noted that the vertical axis of the figure 6 is indicating a unitless factor (per total wind deviation) and to get to the real value of the charging and discharging in MW, the value seen in the figure must be multiplied by the total amounts of the MWs that wind actually deviates (table 1) which can be accessed by the code written to solve the objective function problem.

Table 1 - Total amount of wind deviation in different hours.

70.44426374907874	69.65665001030104	97.37078570814512
63.8897419953434	70.38282228230898	100.80840192672171
65.5176493059037	74.27322381069797	109.62768607595511
70.67842560851214	77.03145816359326	117.02875716898392
74.04023950942	83.74546954486547	111.24839256079292
67.46425256501456	80.16575206776776	104.3594941062782
77.98615084775565	78.36967781356071	109.40164435480203
73.24757852871613	89.14633364913168	108.15730258286914

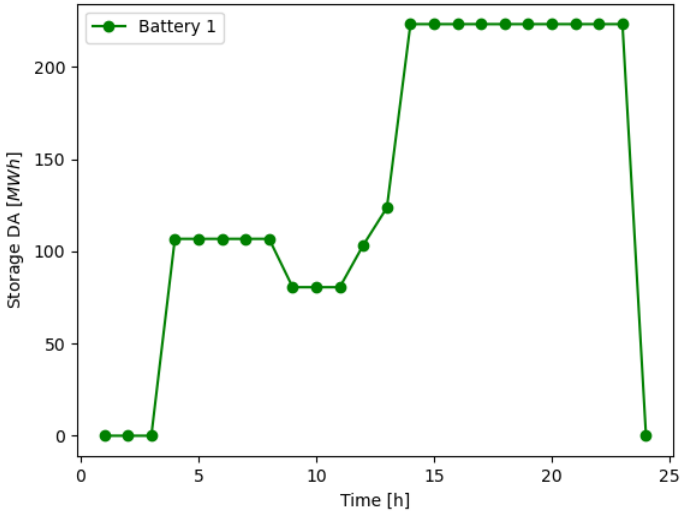

Figure 8– Storage energy state in day-ahead.

Figure 8 shows the storage states in the DA market. As is clear in figure 8, the storage energy state is one of the three following options, upward slope, downward slope, or no slope at all. The upward slope shows the charging state of the storage, while the downward slope indicates the discharging state and lastly, no-slope means that the storage is not participating in the power network during some specific hours.

As shown in the figure below, the storage starts to charge at the hour 4 about 100MW due to the lower market clearing prices which can be seen in figure 4, does not participate in the power network between hours 5 to 8 (neither charge or discharges), discharges at hour 9, and charges gradually between hours 11 and 14 and fully discharges in the last hour again. This figure can be interpreted same as the figure 5 and it is prudent to mention that both figures convey a similar message.

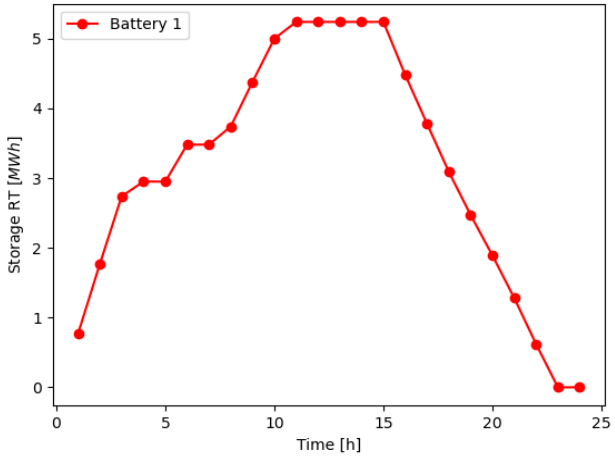

Figure 9– Storage energy state in real-time.

Figure 9 is designated to the storage energy state in real-time market. Similar to the last figure, energy of the storage can be shown in one of three states: an upward slope, a downward slope, or no slope. An upward slope indicates that the storage is charging, while a downward slope indicates that it is discharging. A state with no slope means that the storage is not actively connected to the power network during certain hours. It is prudent to note that as indicated in figure 9's vertical axis the amount of energy charging and discharging in real-time is way less than day-ahead.it can be stated that the storage has much less participation in real-time.

3.3 Sensitivity Analysis

In this section sensitivity analysis will be performed on the important input variables of the problem to see how these variables can impact the output of the model. It should be stated that this analysis will help identify the critical factors that have the most significant impact on the results.

As explained in section 3.1, a baseline case was defined, and the numerical results and the outcomes were investigated. In the baseline case, the selected violation probability is ϵ = 0.1, and the cost of availability for generators (C_g^{Av}) is 100€/MW, while the cost of availability for storage (C_s^{Av}) is 10€/MW. The initial investment cost for implementing the storage (I_s^0), as well as the storage investment cost (I_s^E) and the investment costs related to the maximum storage capacity (I_s^Q), are all fixed at 2€/MW. The binary variable U_s is set to 1, and a large value of 1000 is assigned to the variable M.

In the baseline case, all variables are assumed to be held constant except for the price difference. Subsequently, in the first scenario, the price difference is manipulated to evaluate its impact on the outcomes. The value has been set to 1 (the baseline case), 5 and 10 to have a better resolution on how its increase will alter the outcomes.

As explained earlier in the numerical results section, the power dispatch figure displays the optimized schedule for day-ahead power distribution, which is the result of coordinated efforts between power networks and wind generators in a typical scenario. It can be understood from the figure B1, that by altering the price difference, The power dispatch remains relatively stable and consistent. Figure B2 also indicates that, changing the price difference, would not be able to refashion the outcomes regarding the generator flexibility reserve. Given the direct impact of the price difference on the participation of the storage in day-ahead and real-time, it is sensible that altering the price difference would not affect the generator's participation pattern.

Regarding the storage flexibility reserve (figure B3), it can be noted that at hours 4, 6, 9 and 10, a slight change in flexibility reserve is being observed which can be justified with the slight change in market clearing prices at the very same hours observed in figure B4. It can be observed from the above-mentioned figures, with the increase of the price difference the

flexibility reserve of the storage decreases as this change is resulting in rising MCP at those hours.

Without considering the results of the problem formulation, it was expected to see a reduction in the participation of the storage by increasing the price difference. By looking at figure B5 and B6, it can be stated that in the day-ahead, increasing the price difference is resulting in fewer participation of the storage both in the number of hours that the storage is participating in the power network and the amount of energy that it is charging or discharging. Although it should be mentioned that since the storage participation in real time was not that much even in the baseline case, it doesn't go through change during the price difference alteration and stays stable. This can be also applied to the figures B7 and B8, which are presenting the storage energy state in day-ahead and real-time respectively. As an example, it can be noticed that in figure B7, with the increase of price difference from 1 to 5, the storage state between hours four to nine decreases from more than 100 MW/h to less than 100.

For the second scenario, from the baseline variables the effectiveness of the availability costs of the generators and storage will be discussed. In this scenario, the violation probability that has been chosen is $\epsilon = 0.1$. The costs for initial investment in storage implementation (I_s^0), as well as investment in storage (I_s^E) and investment related to maximum storage capacity (I_s^Q), are all fixed at 2€/MW. The binary variable U_s is set at 1, and a large value of 1000 is assigned to the variable M.

The second scenario will include three different situations in which the storage availability cost is less than the generator availability cost, the availability costs in both the generators and the storage is equal, and the last one where the storage availability cost is greater than the generator. As explained in the baseline case defining section, in the baseline case one of the reasons that the storage availability cost was considered to be less than the generators, was the fact that it ensures participation of the storage in the power network. If the storage availability cost is greater than the generator's it doesn't make sense for the whole system to take the generator into account and will work with the generator's participation only since it is going to cost less. Therefore, it is expected to observe less participation from the storage as its availability cost grows.

Based on figures B10 and B11 and as expected by setting a greater or equal value for the storage availability cost than the generator's, we are noticing less participation from the storage side and as observed in the generator flexibility reserve figure (figure B10), the whole wind power deviation deficit is covered by the generators and after equality of the available costs the storage's participation stops (figure B11). With a similar argument and considering the figures B13 and B14, It can be stated that by increasing the availability cost of the storage, its participation both in day-ahead and real time stops. Looking more precisely at the figure B13 shows a significant decrease both in the times and amount of storage participation in day-ahead, which can also be complemented by considering figure B15. As mentioned earlier and in the baseline case, it was clear that the storage does not play a great role in the real-time and the participation is not that impressive. Here again in scenario 2, after manipulation of the

availability costs the storage participation becomes zero as soon as the availability cost of the storage is set to be equal to the generator (figure 14 and 16).

To end the second scenario, it should be stated that as shown in figure B9, the scheduled DA power dispatch does not change remarkably. Since in the third situation the availability cost of generators is lowered from 100 €/MW to 10 €/MW, it is sensible to have more power dispatch covered by the conventional generators due to the less cost.

Lastly, in the third scenario, the investment costs are manipulated to observe the result of the problem formulation and have a clear perspective on their effects on the outcomes. The scenario is defined in a way that the violation probability (ϵ), has been chosen to be equal to 0.1. the availability cost for generators (C_g^{Av}) and the storage (C_s^{Av}) are back to the initial value of 100€/MW and 10€/MW respectively. The binary value U_s remains equal to one and M is 1000.

To see the effect of the investment costs, the sensitivity analysis of the third scenario is divided into three different situations, first the one in which all the investment costs are equal to 2€/MW (baseline case), second the one where all of the investment costs are set to 4€/MW, and the last situation where all of the costs are 1€/MW. The goal of the analysis is to observe the changes as the investment prices fluctuate.

Regarding the DA power dispatch (figure B17), except for hours 4 to 6 and the last hours of the day, there is not much of a significant change. While in figure B18 and figure B19, it is noticeable that by increasing the investment costs the participation of the storage will stop and the wind deviation deficit will be compensated by the generators only which can be understood by looking at the constraint 4m. These two figures indicate that by lowering the investment costs, the participation of the storage will grow both regarding the amount and the times in a day (situation three in which the investment costs are all set to 1€/MW).

Figure B20 specifies that the alteration of the investment costs would have a difference in the market clearing price. As shown in the figure, by both increasing and decreasing the costs the MCP figure has gone through some changes in different hours.

Concerning the amount and the number of times that the storage participates in DA and RT, as stipulated by the figures B21, B22, B23 and B24, by enlarging the investment costs, the participation of the storage stops both in DA and real-time. While the costs decrease, the participation amount and multiplicity grow. Looking at the third situation in all the figures, as mentioned earlier, in more depth, it can be noted that even in real-time, we will be facing more storage participation.

In this section, the sensitivity analysis of three different scenarios was examined. To summarize the findings, it can be stated that increasing the price difference and the investment cost would result in less storage participation. It should also be noted that storage participation is guaranteed only when the storage availability cost is less than the generators' availability cost. The participation will stop as soon as it gets close or equal to the generators. Considering what

has been stated in this section, the next section will be dedicated to the result and conclusion to the research question.

4 Conclusion

The thesis aimed to propose an efficient method for scheduling and operating a power system with the presence of single storage. To accomplish this, the study suggested utilizing a market clearing mechanism that incorporates distributed robust chance constraint (DRCC) methods for short-term operations to solve the operational problem of storage. These DRCC methods help to manage the risk associated with the uncertainty of flexible technologies. The problem at hand assumes a market setup where competition is fully centralized. The goal is to optimize utility within the power sector, while also accounting for the presence of a storage system. It is important to maintain flexibility to compensate for any potential power imbalances that may arise at a later stage, while still achieving the optimal outcome.

It should be noted that by assuming the response to uncertainty is affine, the suggested approach allows the market operator to identify the most effective plan for executing flexibility. This plan aims to maximize social welfare in the day-ahead market, while also managing any potential power imbalances that could result from the worst-case probability distribution in real-time operations. The term "availability costs" is used to define the market positioning of flexible assets both for generators and storage, as well as to regulate how these assets are dispatched. By taking into account these costs, the dispatch mechanism can effectively manage the availability of flexible assets and ensure that they are utilized efficiently in meeting the demands of the market. With the coordination mechanism proposed in the study, it becomes possible to use the short-term flexibility that is inherent in the storage system. This is achieved by implementing intelligent operations within the power network and through its integration with the storage system.

The findings of the study demonstrate that the suggested method makes it possible for the market operator to enhance social welfare by taking advantage of the synergies that exist between interconnected power networks and storage, particularly in situations where renewable energy generation is uncertain.

Furthermore, it was found that the model is sensitive to the choice of price differences, availability costs of the generator and storage, and the investment costs related to both generator and the storage, and under the provided assumptions and constraints can lead to a higher utility which supports the hypothesis of the strategic market participation of an energy storage system in a competitive market.

In the end, building an energy storage system to provide flexibility response under the assumptions that were explained before, cannot be precisely advised since there are many assumptions along the way to get to the desired conclusion.

5 Future Works

This section identifies some remaining challenges that need to be addressed in future research. This suggests that further investigation is necessary to better understand the complexities of the issue and develop more comprehensive solutions.

First, to strengthen the robustness of the results and verify the effectiveness of the proposed model and implemented code, it would be beneficial to conduct a more extensive evaluation over an extended period, such as 10 consecutive days. Such an investigation would provide additional evidence of the ability of the storage system to actively participate in the power network and its associated operations.

Then, there is a potential avenue for further research that involves examining ways in which the storage system can generate revenue and offset investment costs through energy trading. This could be accomplished by extending the proposed framework to incorporate an analysis of infrastructure investment decisions, thereby providing a more comprehensive understanding of the financial implications and trade-offs of the approach.

References

Alskaif, T., Crespo-Vazquez, J. L., Sekuloski, M., van Leeuwen, G., & Catalao, J. P. S. (2022). Blockchain-Based Fully Peer-to-Peer Energy Trading Strategies for Residential Energy Systems. *IEEE Transactions on Industrial Informatics*, *18*(1), 231–241. https://doi.org/10.1109/TII.2021.3077008

Azari, D., Shariat Torbaghan, S., Cappon, H., Keesman, K. J., Rijnaarts, H., & Gibescu, M. (2019). Exploring the impact of data uncertainty on the performance of a demand response program. *Sustainable Energy, Grids and Networks*, *20*, 100262. https://doi.org/10.1016/J.SEGAN.2019.100262

Azari, D., Torbaghan, S. S., Cappon, H., Keesman, K. J., Gibescu, M., & Rijnaarts, H. (2020). On the Sensitivity of Local Flexibility Markets to Forecast Error: A Bi-Level Optimization Approach. *Energies 2020, Vol. 13, Page 1959*, *13*(8), 1959. https://doi.org/10.3390/EN13081959

Bezanson, J., Edelman, A., Karpinski, S., & Shah, V. B. (2017). Julia: A Fresh Approach to Numerical Computing. *Https://Doi.Org/10.1137/141000671*, *59*(1), 65–98. https://doi.org/10.1137/141000671

Boyd, S., Parikh, N., Chu, E., Peleato, B., & Eckstein, J. (2011). Distributed Optimization and Statistical Learning via the Alternating Direction Method of Multipliers. *Foundations and Trends® in Machine Learning*, *3*(1), 1–122. https://doi.org/10.1561/2200000016

Chio, C., Sain, M., & Qin, W. (2019). Lignin utilization: A review of lignin depolymerization from various aspects. *Renewable and Sustainable Energy Reviews*, *107*, 232–249. https://doi.org/10.1016/J.RSER.2019.03.008

Denholm, P., Ela, E., Kirby, B., & Milligan, M. (2010). *The Role of Energy Storage with Renewable Electricity Generation*. http://www.osti.gov/bridge

di Silvestre, M. L., Favuzza, S., Riva Sanseverino, E., & Zizzo, G. (2018). How Decarbonization, Digitalization and Decentralization are changing key power infrastructures. *Renewable and Sustainable Energy Reviews*, *93*, 483–498. https://doi.org/10.1016/j.rser.2018.05.068

Dunning, I., Huchette, J., & Lubin, M. (2015). JuMP: A Modeling Language for Mathematical Optimization. *SIAM Review*, *59*(2), 295–320. https://doi.org/10.1137/15M1020575

Dunning, I., Huchette, J., & Lubin, M. (2017). JuMP: A Modeling Language for Mathematical Optimization. *Https://Doi.Org/10.1137/15M1020575*, *59*(2), 295–320. https://doi.org/10.1137/15M1020575

Energy Agency, I. (2020). *World Energy Outlook 2020*. www.iea.org/weo

Geels, F. W. (2002). Technological transitions as evolutionary reconfiguration processes: a multi-level perspective and a case-study. *Research Policy*, *31*(8–9), 1257–1274. https://doi.org/10.1016/S0048-7333(02)00062-8

Godoy Simões, M., Roche, R., Kyriakides, E., Suryanarayanan, S., Blunier, B., McBee, K., Nguyen, P., Ribeiro, P., & Miraoui, A. (2014). Comparison of smart grid technologies and progress in the USA and Europe. *Green Energy and Technology*, *0*(9781447162803), 221–238. https://doi.org/10.1007/978-1-4471-6281-0_11

Grainger, J. J., & Stevenson, W. D. (1994). *POWER SYSTEM ANALYSIS*. New York: McGraw-Hill.

Gritsenko, D. (2018). Explaining choices in energy infrastructure development as a network of adjacent action situations: The case of LNG in the Baltic Sea region. *Energy Policy*, *112*, 74–83. https://doi.org/10.1016/J.ENPOL.2017.10.014

Hull, J. C., Rotman, J. L., Hall, P., Columbus, B., New, I., San, Y., Upper, F., River, S., Cape, A., Dubai, T., Madrid, L., Munich, M., Montreal, P., Delhi, T., Saõ, M. C., Sydney, P., Kong, H., Singapore, S., & Tokyo, T. (n.d.). *OPTIONS, FUTURES, AND OTHER DERIVATIVES Maple Financial Group Professor of Derivatives and Risk Management*. http://www.pearsoned.com/legal/permission.htm.

Jordan, M., Kleinberg, J., & Schölkopf, B. (2006). *Pattern Recognition and Machine Learning*.

Katiraei, F., Iravani, R., Hatziargyriou, N., & Dimeas, A. (2008). Microgrids management. *IEEE Power and Energy Magazine*, *6*(3), 54–65. https://doi.org/10.1109/MPE.2008.918702

Kundur, P. (1994). Power System Stability and Control. In *New York: McGraw-Hill*.

le Cadre, H., Jacquot, P., Wan, C., & Alasseur, C. (2020). Peer-to-peer electricity market analysis: From variational to Generalized Nash Equilibrium. *European Journal of Operational Research*, *282*(2), 753–771. https://doi.org/10.1016/J.EJOR.2019.09.035

Luo, X., Dooner, M., He, W., Wang, J., Li, Y., Li, D., & Kiselychnyk, O. (2018). Feasibility study of a simulation software tool development for dynamic modelling and transient control of adiabatic compressed air energy storage with its electrical power system applications. *Applied Energy*, *228*, 1198–1219. https://doi.org/10.1016/J.APENERGY.2018.06.068

Luo, X. J., Oyedele, L. O., Akinade, O. O., & Ajayi, A. O. (2020). Two-stage capacity optimization approach of multi-energy system considering its optimal operation. *Energy and AI*, *1*, 100005. https://doi.org/10.1016/J.EGYAI.2020.100005

Mengelkamp, E., Notheisen, B., Beer, C., Dauer, D., & Weinhardt, C. (2018). A blockchain-based smart grid: towards sustainable local energy markets. *Computer Science - Research and Development*, *33*(1–2), 207–214. https://doi.org/10.1007/S00450-017-0360-9/TABLES/1

Mitridati, L., Kazempour, J., & Pinson, P. (2020). Heat and electricity market coordination: A scalable complementarity approach. *European Journal of Operational Research*, *283*(3), 1107–1123. https://doi.org/10.1016/J.EJOR.2019.11.072

Oconnell, N., Pinson, P., Madsen, H., & Omalley, M. (2014). Benefits and challenges of electrical demand response: A critical review. *Renewable and Sustainable Energy Reviews*, *39*, 686–699. https://doi.org/10.1016/J.RSER.2014.07.098

Ordoudis, C., Pinson, P., & Morales, J. M. (2019). An Integrated Market for Electricity and Natural Gas Systems with Stochastic Power Producers. *European Journal of Operational Research*, *272*(2), 642–654. https://doi.org/10.1016/J.EJOR.2018.06.036

Pourmousavi, S. A., Nehrir, M. H., & Sharma, R. K. (2015). Multi-Timescale Power Management for Islanded Microgrids Including Storage and Demand Response. *IEEE Transactions on Smart Grid*, *6*(3), 1185–1195. https://doi.org/10.1109/TSG.2014.2387068

Ramos, A., de Jonghe, C., Gómez, V., & Belmans, R. (2016). Realizing the smart grid's potential: Defining local markets for flexibility. *Utilities Policy*, *40*, 26–35. https://doi.org/10.1016/j.jup.2016.03.006

Ratha, A., Schwele, A., Kazempour, J., Pinson, P., Torbaghan, S. S., & Virag, A. (2020). Affine Policies for Flexibility Provision by Natural Gas Networks to Power Systems. *Electric Power Systems Research*, *189*, 106565. https://doi.org/10.1016/J.EPSR.2020.106565

Schwele, A., Arrigo, A., Vervaeren, C., Kazempour, J., & Vallée, F. (2020). Coordination of Electricity, Heat, and Natural Gas Systems Accounting for Network Flexibility Coordination of Electricity, Heat, and Natural Gas Systems Accounting for Network Flexibility. *Citation*, *189*. https://doi.org/10.1016/j.epsr.2020.106776

Shariat Torbaghan, S., Madani, M., Sels, P., Virag, A., le Cadre, H., Kessels, K., & Mou, Y. (2021). Designing day-ahead multi-carrier markets for flexibility: Models and clearing algorithms. *Applied Energy*, *285*, 116390. https://doi.org/10.1016/J.APENERGY.2020.116390

Shiller, R. J. (2015). Irrational Exuberance: Revised and Expanded Third edition. *Princeton University Press*.

Sorin, E., Bobo, L., & Pinson, P. (2018). *Consensus-based approach to peer-to-peer electricity markets with product differentiation*. http://arxiv.org/abs/1804.03521

Stagg, G. W., & el Abiad, A. H. (n.d.). *Computer Methods In Power System Analysis* (student edition). Retrieved February 27, 2023, from https://www.academia.edu/34684627/Computer_Methods_In_Power_System_Analysis_by_G_W_Stagg_and_A_H_El_Abiad

Torbaghan, S. S., Blaauwbroek, N., Kuiken, D., Gibescu, M., Hajighasemi, M., Nguyen, P., Smit, G. J. M., Roggenkamp, M., & Hurink, J. (2018). A market-based framework for demand side flexibility scheduling and dispatching. *Sustainable Energy, Grids and Networks*, *14*, 47–61. https://doi.org/10.1016/J.SEGAN.2018.03.003

Torbaghan, S. S., Suryanarayana, G., Hoschle, H., D'Hulst, R., Geth, F., Caerts, C., & van Hertem, D. (2020). Optimal Flexibility Dispatch Problem Using Second-Order Cone Relaxation of AC Power Flows. *IEEE Transactions on Power Systems*, *35*(1), 98–108. https://doi.org/10.1109/TPWRS.2019.2929845

Tushar, W., Member, S., Saha, T. K., Yuen, C., Smith, D., & Vincent Poor, H. (2020). *Peer-to-Peer Trading in Electricity Networks: An Overview*.

van Leeuwen, G., AlSkaif, T., Gibescu, M., & van Sark, W. (2020). An integrated blockchain-based energy management platform with bilateral trading for microgrid communities. *Applied Energy*, *263*, 114613. https://doi.org/10.1016/J.APENERGY.2020.114613

Weron, R. (2014). Electricity price forecasting: A review of the state-of-the-art with a look into the future. In *International Journal of Forecasting* (Vol. 30, Issue 4, pp. 1030–1081). Elsevier B.V. https://doi.org/10.1016/j.ijforecast.2014.08.008

Wood, A. J., Wollenberg, B. F., & Sheblé, G. B. (2013). *Power generation, operation, and control.* (3rd ed.). Wiley Interscience. https://www.perlego.com/book/1003657/power-generation-operation-and-control-pdf

Appendix A

This section will comprehensively investigate and analyze various potential approaches and methods for addressing the specified issue to identify and select the most effective and feasible solutions. Through thorough examination and evaluation, this study aims to provide valuable insights and recommendations to inform future research and decision-making processes. As explained, there are different methods to tackle the issue in the thesis, and write the constraints based on those discussed in this section.

It is important to note that the methods presented in this section merely represent distinct perspectives on the problem without altering essential assumptions. The inclusion of these methods serves as a guide for further research endeavors.

Constraints in engineering design problems can guarantee that the design satisfies performance, safety, or regulatory criteria, while in resource allocation problems, constraints can restrict the utilization of resources. In machine learning, constraints can assist in avoiding overfitting and ensuring that solutions generalize well to new data (Bishop, 2006). The role of constraints in optimization problems is crucial because they allow optimization algorithms to generate solutions that comply with real-world constraints and necessities. The initial implementations of the DRCC constraint for the storage encountered the occurrence of both charging and discharging simultaneously in both day-ahead and real-time; therefore, various methods for addressing the problem will now be examined to understand better how the DRCC constraints were formulated in this thesis.

By considering Figure B1 and the first method, it can be observed that the storage has undergone charging in day-ahead and has been charged by $\hat{q}_{s,t}^{ch}$. To charge the storage again in real-time, the maximum amount that can be charged is equal to $\overline{Q_s} - \hat{q}_{s,t}^{ch}$, which is demonstrated in the figure. On the other hand, if the battery only discharges in real-time, it can only discharge the amount that has been gained in the day-ahead, which is equal to $\hat{q}_{s,t}^{ch}$. The problem that arises is deciding whether the constraints should be written as explained or whether the storage should be charged and discharged simultaneously. It should be noted that the utilization of this method can be perplexing at various levels, particularly when considering the necessity for the constraints to work and hold with high probabilities. Furthermore, this method may lead to outcomes that differ from expected.

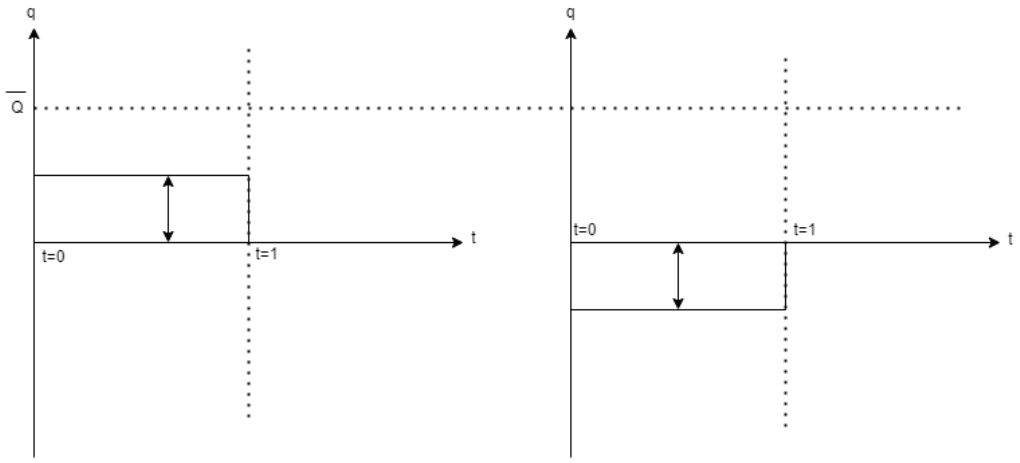

Figure A2 - method one diagram (storage charging and discharging) - the left diagram shows the charging in DA, and the right one shows discharging in RT.

Given the aforementioned reason and the desire to eliminate confusion, the issue will be approached from a new perspective. Method two proposes that the amount of charging that occurred in the day ahead has been restricted in real-time. As the storage can only be charged up to $\hat{q}_{s,t}^{ch}$, the maximum amount of power it can obtain in real-time is equivalent to $\overline{Q_s} - \hat{q}_{s,t}^{ch}$. The theoretical foundation of method two is demonstrated through a simplistic diagram as depicted in Figure B2.

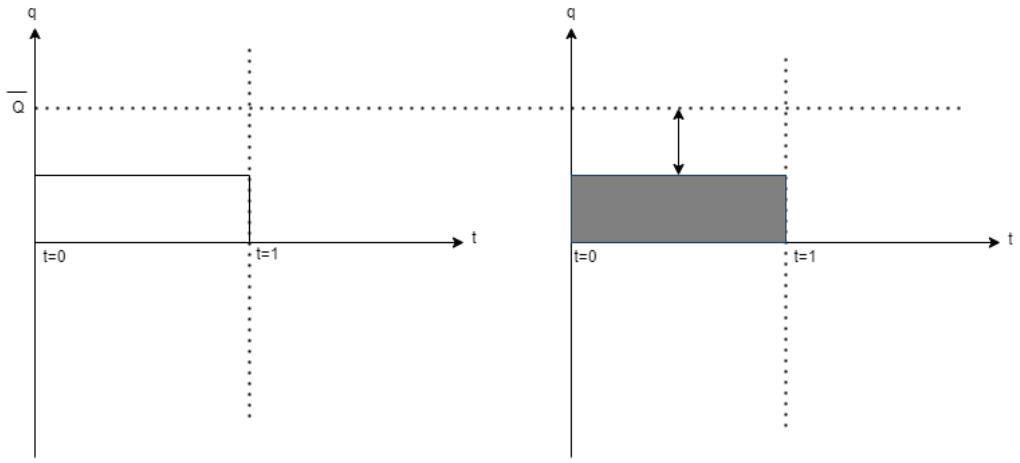

Figure B2 - method two diagram (storage charging and discharging) - the left diagram shows the charging in DA, and the right one shows the amount of power blocked in RT.

Method one and method two are distinguished by a notable variation in their approaches towards the storage's charged power during the real-time period. In method one, said power obtains a negative value during this period, while in method two, it is blocked and prevented from being utilized. Despite the apparent differences between the two methods,

they share a common underlying logic that can be observed through different perspectives. However, a detailed understanding of each method is crucial, as this can affect the performance and outcomes of the given system.

It is prudent to mention that the problem with these methods is the fact that either the implemented constraints based on them result in charging and discharging simultaneously in real-time, or they are unable to capture reality as it actually is.

To circumvent the issues previously mentioned, a modified problem formulation is proposed, wherein method 3 incorporates a distinct approach. In this method, a singular variable q is defined to account for the real-time activity of the storage, with its values potentially fluctuating between positive and negative.

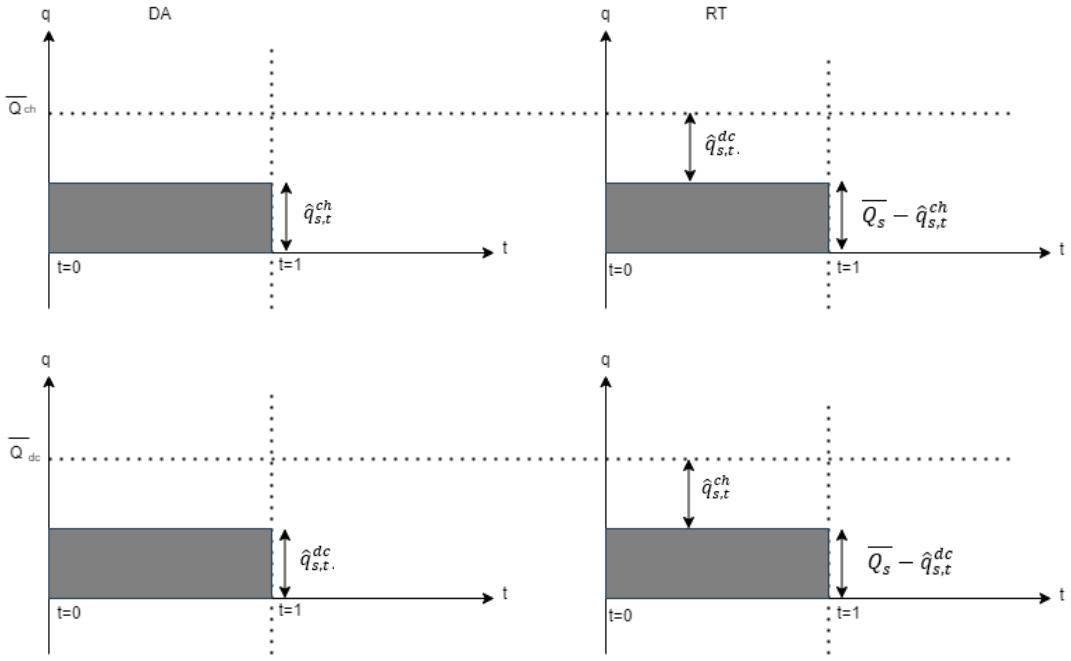

Figure B3 - method three diagrams (storage charging and discharging) – the two left-side diagrams show the storage state in DA, while the two right-side diagrams show the storage state in RT. The upper diagrams indicate the storage while charging while the two bottom diagrams indicate the storage state while discharging.

Regarding figure B3, it can be understood that in case the storage charges $\hat{q}^{ch}_{s,t}$ in DA, and discharged $\hat{q}^{dc}_{s,t}$, the amount of power that can be charged or discharged in real-time is bound as below:

$$-\hat{q}^{dc}_{s,t} \leq \breve{q}^{ch}_{s,t} \leq \left(\overline{Q_s} - \hat{q}^{ch}_{s,t}\right) \qquad \text{(M3.1)}$$

$$-\hat{q}^{ch}_{s,t} \leq \breve{q}^{dc}_{s,t} \leq \left(\overline{Q_s} - \hat{q}^{dc}_{s,t}\right) \qquad \text{(M3.2)}$$

The two inequalities above, show the limitation of the amount that the storage can charge ($\breve{q}_{s,t}^{ch}$) and discharge ($\breve{q}_{s,t}^{dc}$) in real-time. Inequality (M3.1) shows that the amount of power that the storage can be charged should not exceed from the remaining capacity of the storage from the day-ahead; and, it must be at least equal to the amount of the power that has been discharged from the storage in day-ahead to prevent the storage to end-up with a negative value which does not map the reality. The same logic can apply to the inequality (M3.2) while the storage is discharging in real-time. It should be mentioned that the inequalities (2h), (2i), (4h) and (4i) are driven from this method.

Finally, it is worth noting that with sufficient research and contemplation, alternative methods (method one and method two) could also prove effective. The key factor lies in devising an approach that accurately captures the reality of the situation, and appropriately formulating the constraints to reflect this.

Appendix B

In this appendix, the results of the sensitivity analysis conducted for the proposed model are presented.

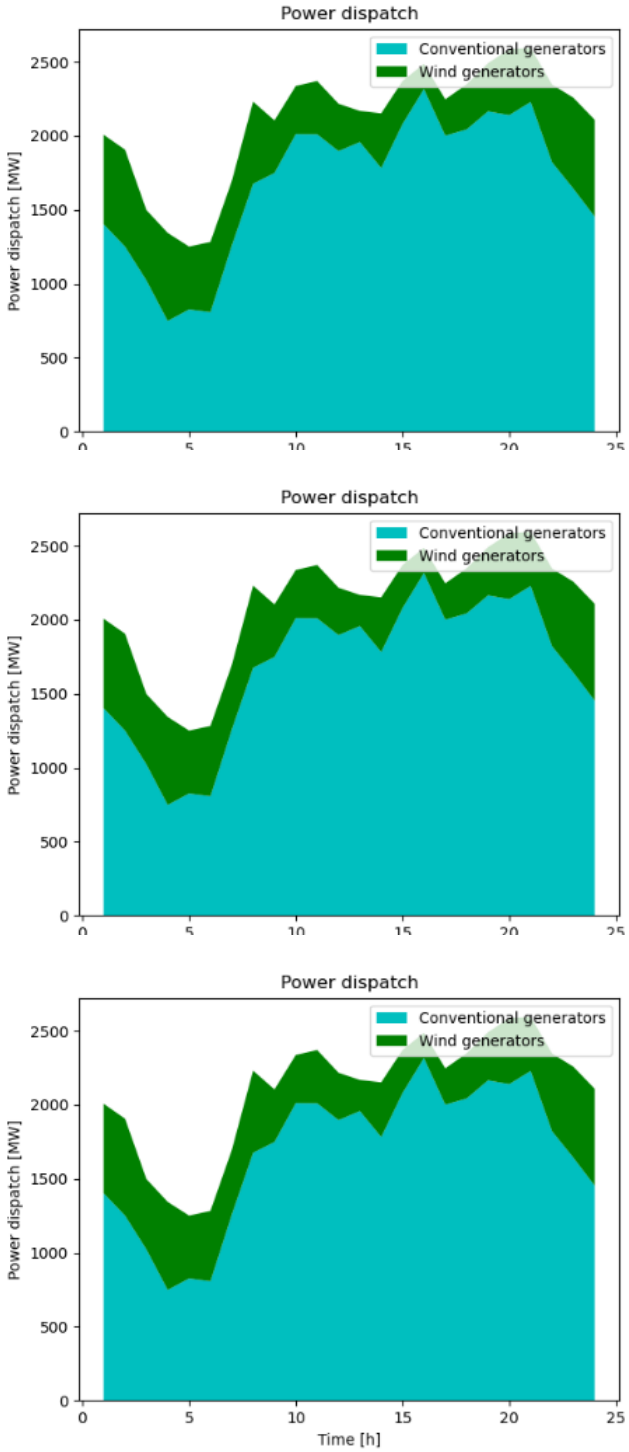

Figure B1– Scheduled DA power dispatch. The Top figure's price difference is set to 1, the middle one is set to 5 and the bottom is set to 10.

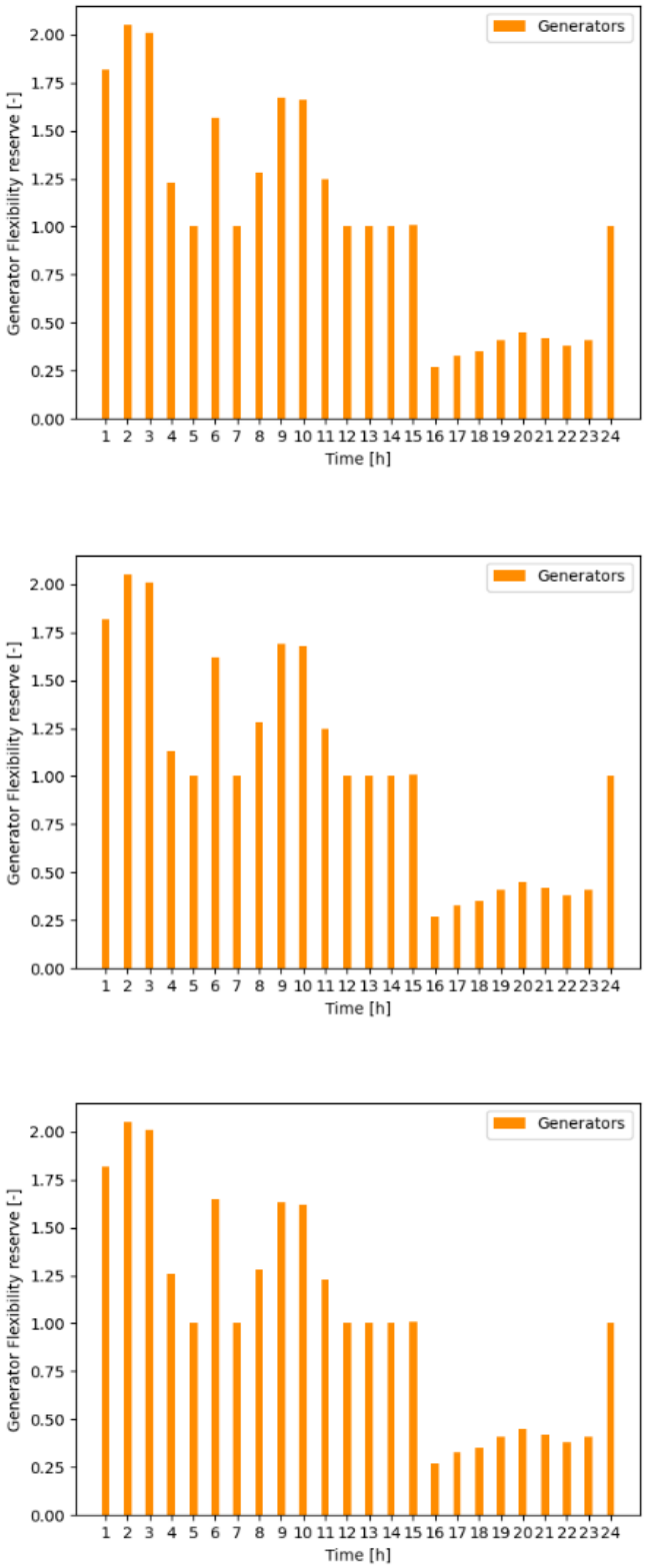

Figure B2– Generator Flexibility Reserve. The top figure's price difference is set to 1, the middle one is set to 5 and the bottom is set to 10.

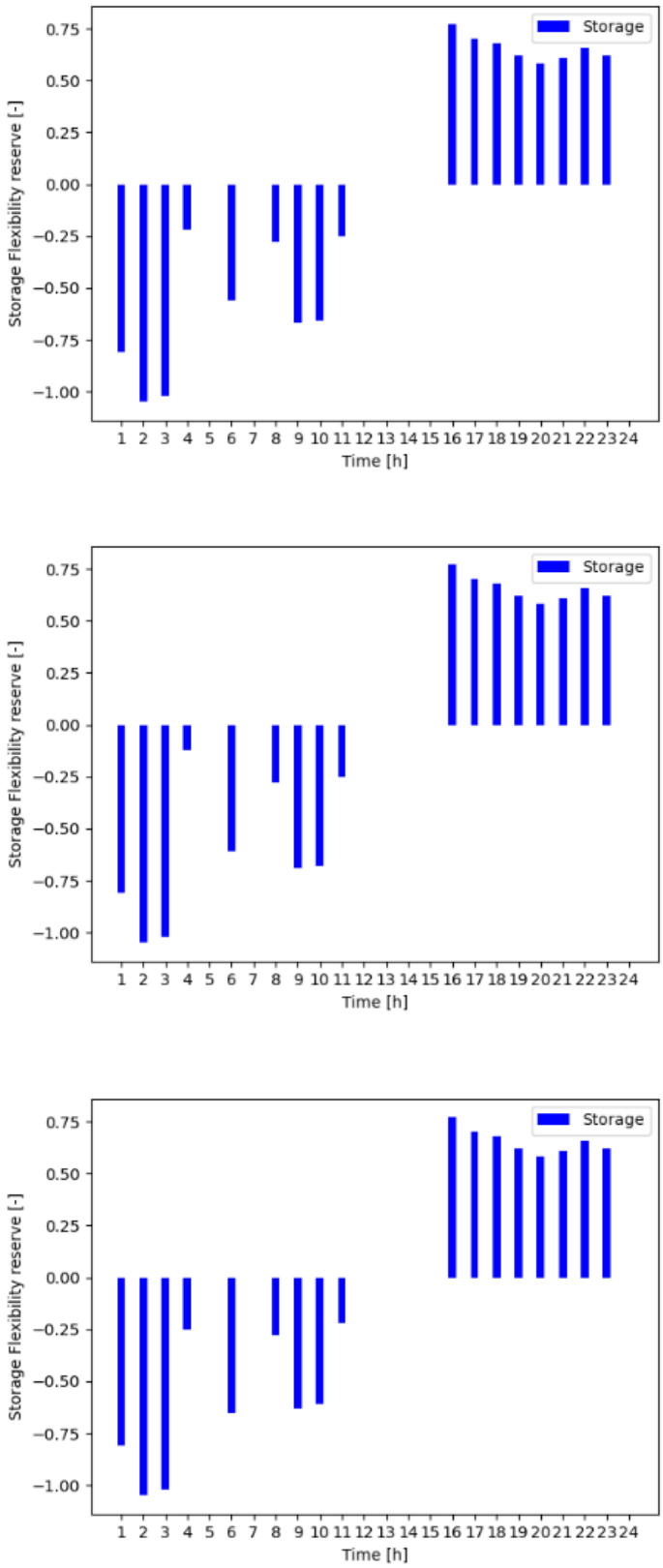

Figure B3 – Storage Flexibility Reserve. The top figure's price difference is set to 1, the middle one is set to 5 and the bottom is set to 10.

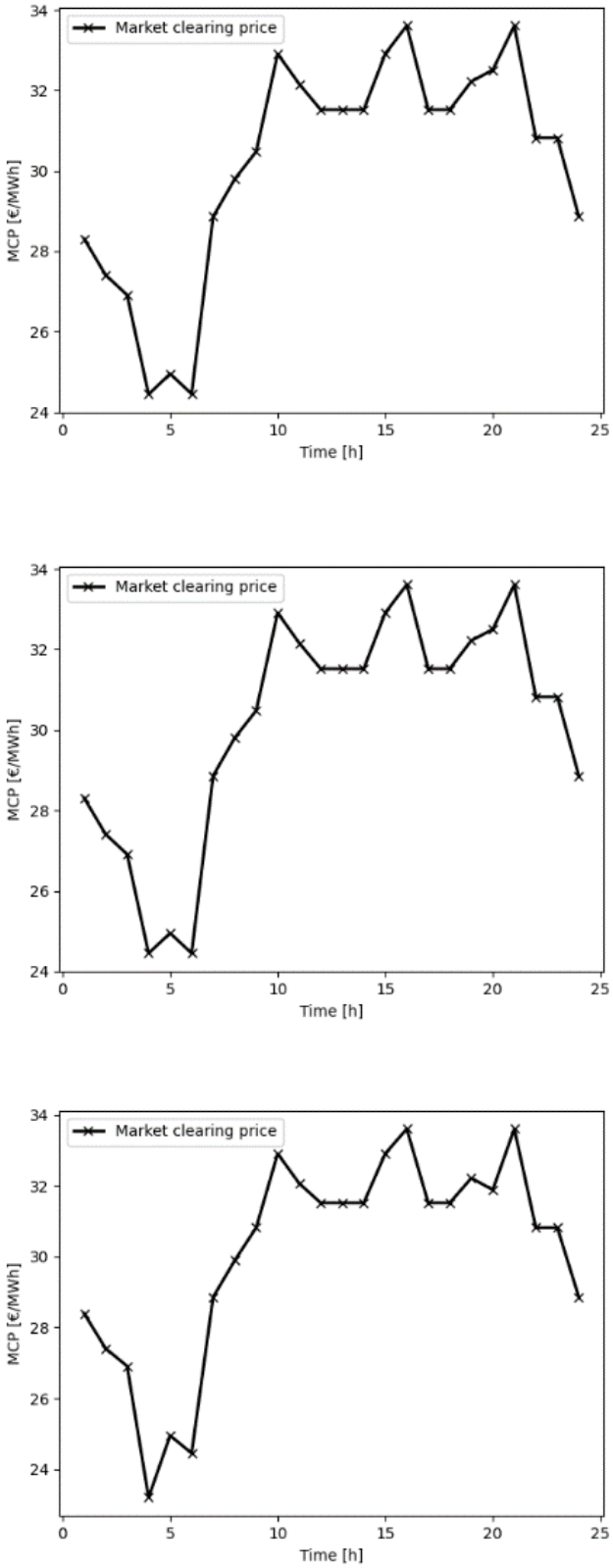

Figure B4 – Market clearing price. The top figure's price difference is set to 1, the middle one is set to 5 and the bottom is set to 10.

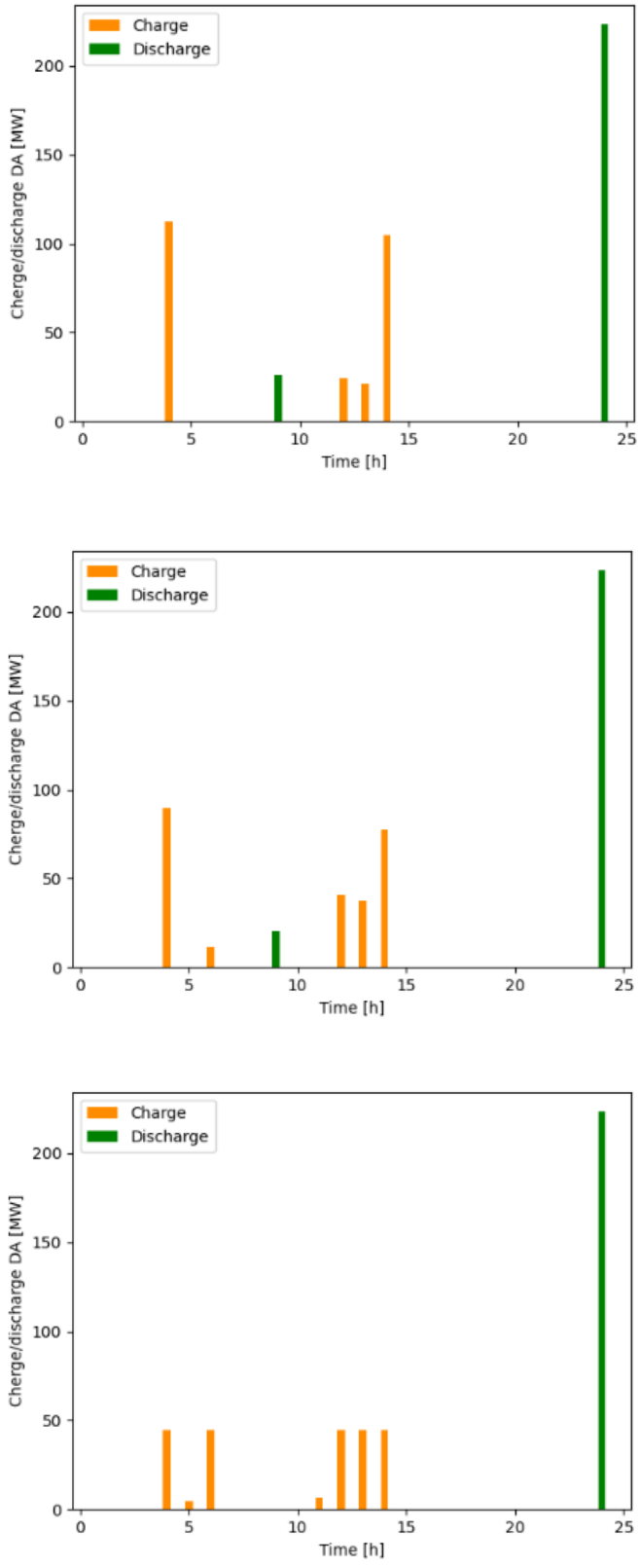

Figure B5 – Day-ahead Charging and discharging of the storage. The top figure's price difference is set to 1, the middle one is set to 5 and the bottom is set to 10.

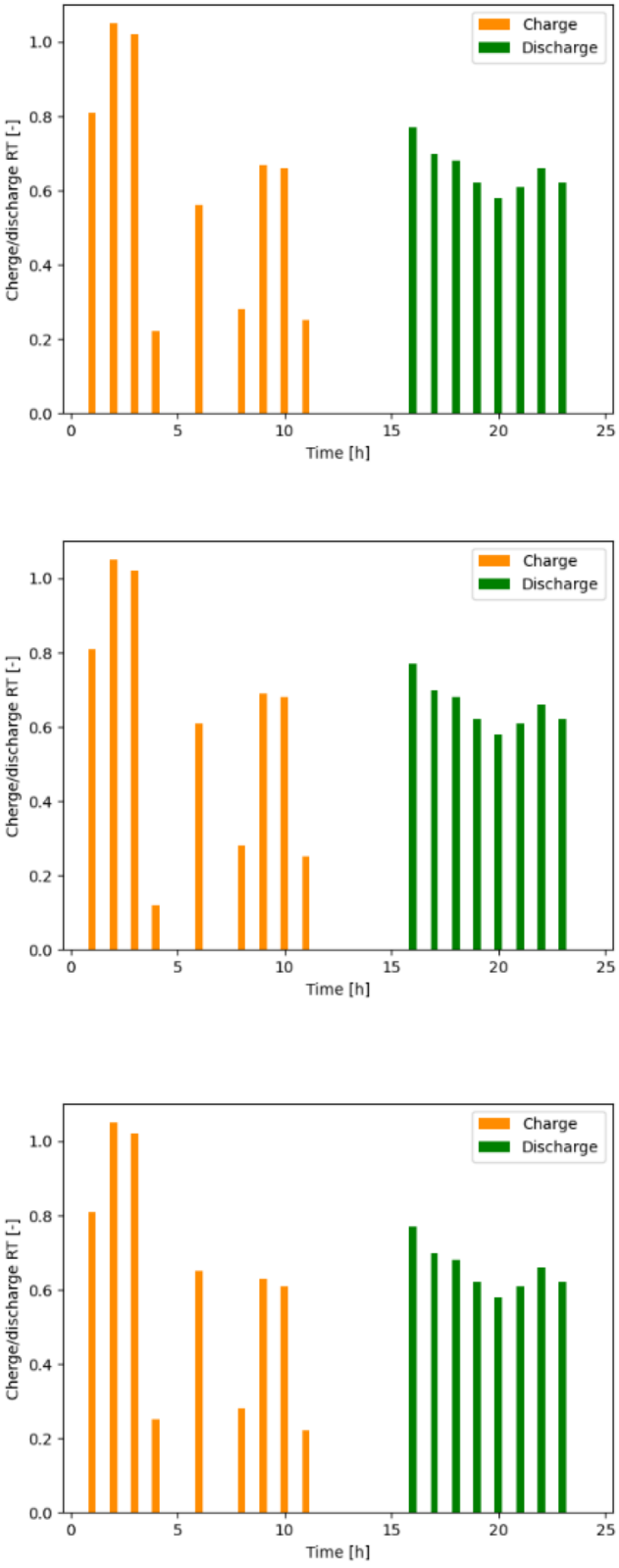

Figure B6 – Real-time Charging and discharging of the storage. The top figure's price difference is set to 1, the middle one is set to 5 and the bottom is set to 10.

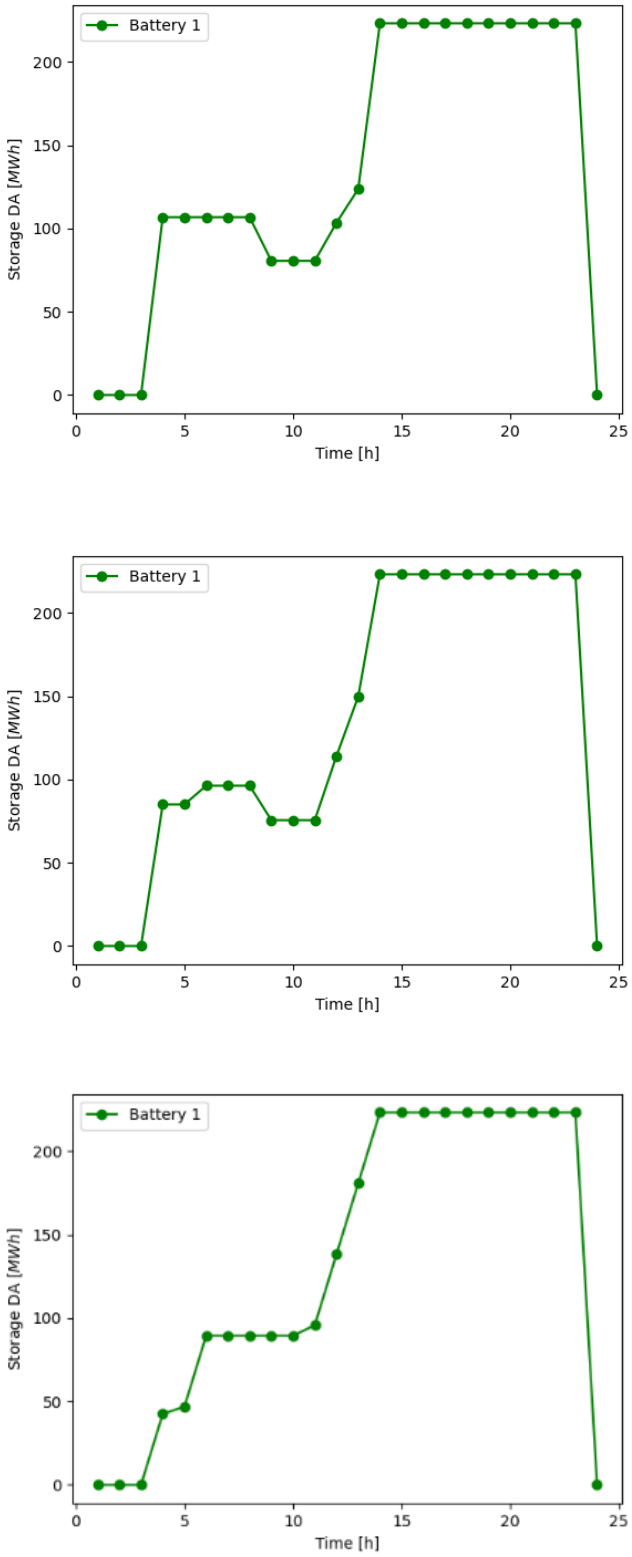

Figure B7 – Storage energy state in day-ahead. The top figure's price difference is set to 1, the middle one is set to 5 and the bottom is set to 10.

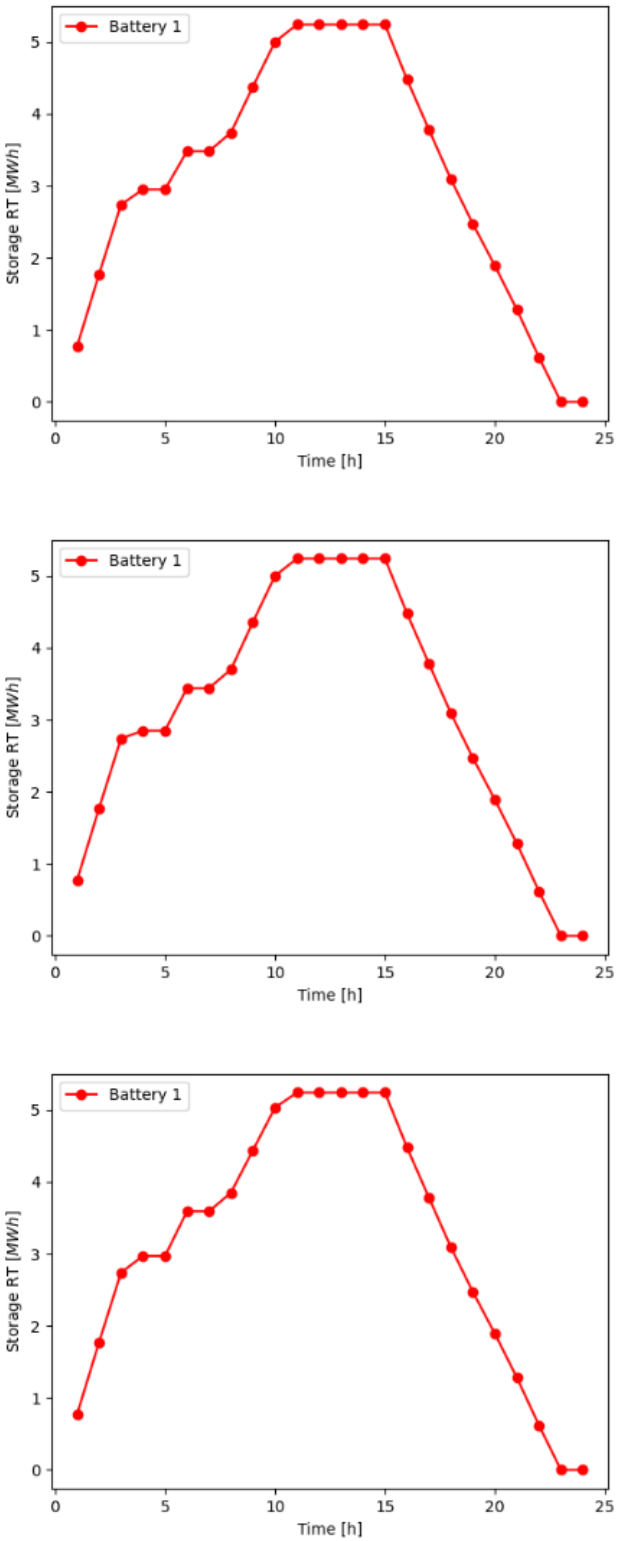

Figure B8 – Storage energy state in Real-time. The top figure's price difference is set to 1, the middle one is set to 5 and the bottom is set to 10.

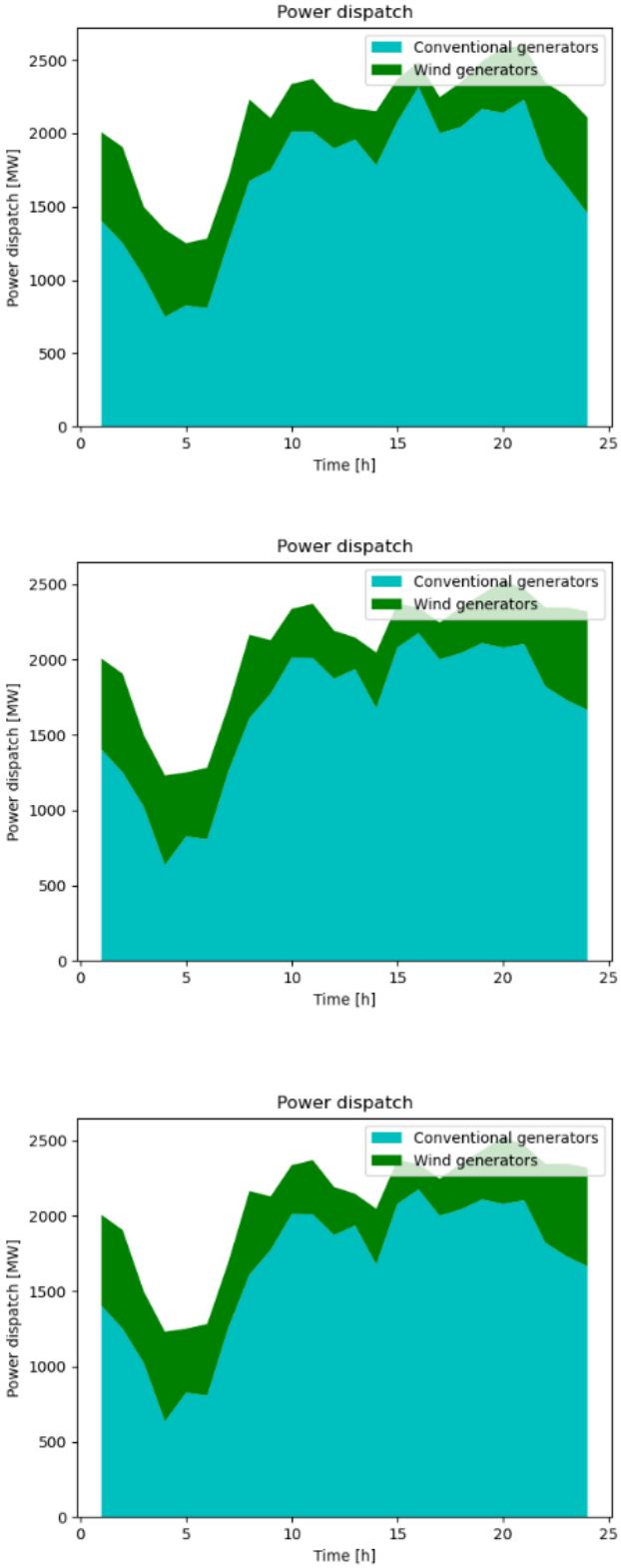

Figure B9– Scheduled DA power dispatch. In the top figure the availability cost of the storage is considered to be less than generator, in the middle figure the availability cost of storage and generators are equal and in the bottom figure the availability cost of storage is set to be less than the availability cost of the generator.

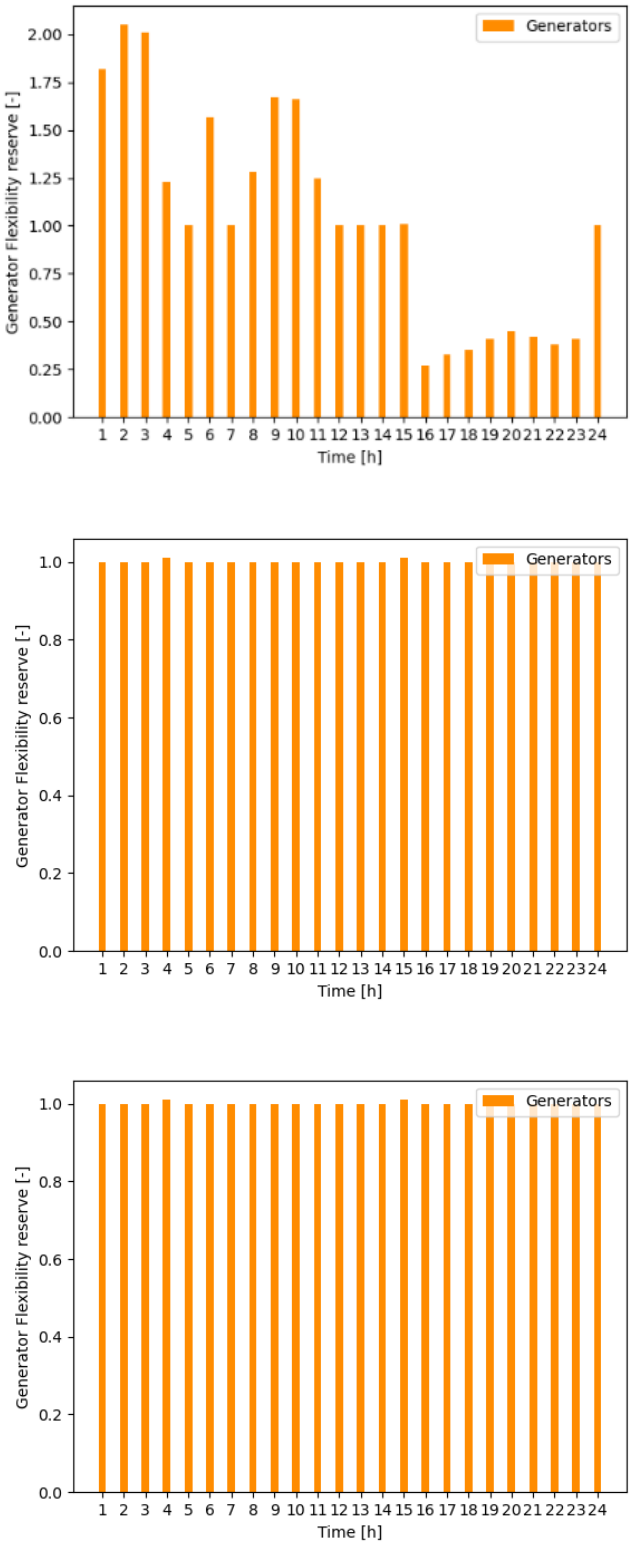

Figure B10– Generator Flexibility Reserve. In the top figure the availability cost of the storage is considered to be less than generator, in the middle figure the availability cost of storage and generators are equal and in the bottom figure the availability cost of storage is set to be less than the availability cost of the generator.

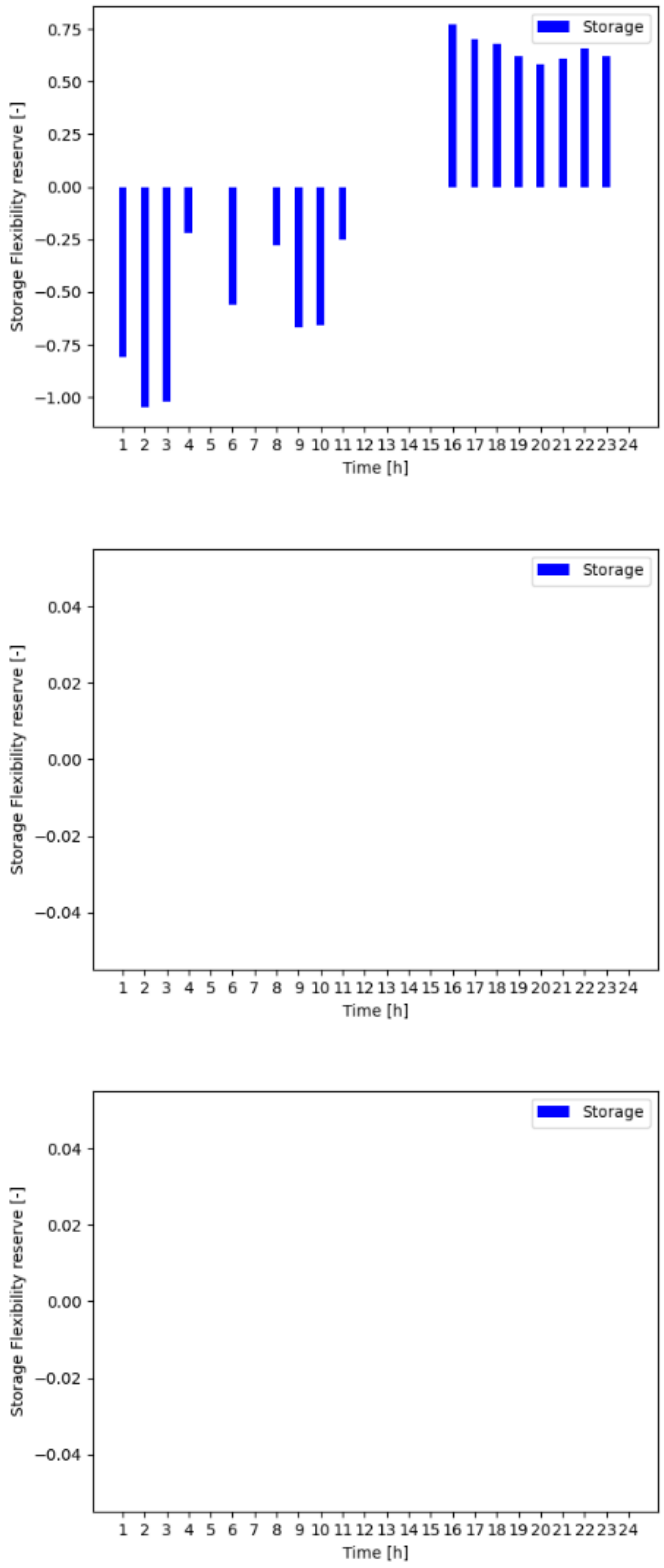

Figure B11– Storage Flexibility Reserve. In the top figure the availability cost of the storage is considered to be less than generator, in the middle figure the availability cost of storage and generators are equal and in the bottom figure the availability cost of storage is set to be less than the availability cost of the generator.

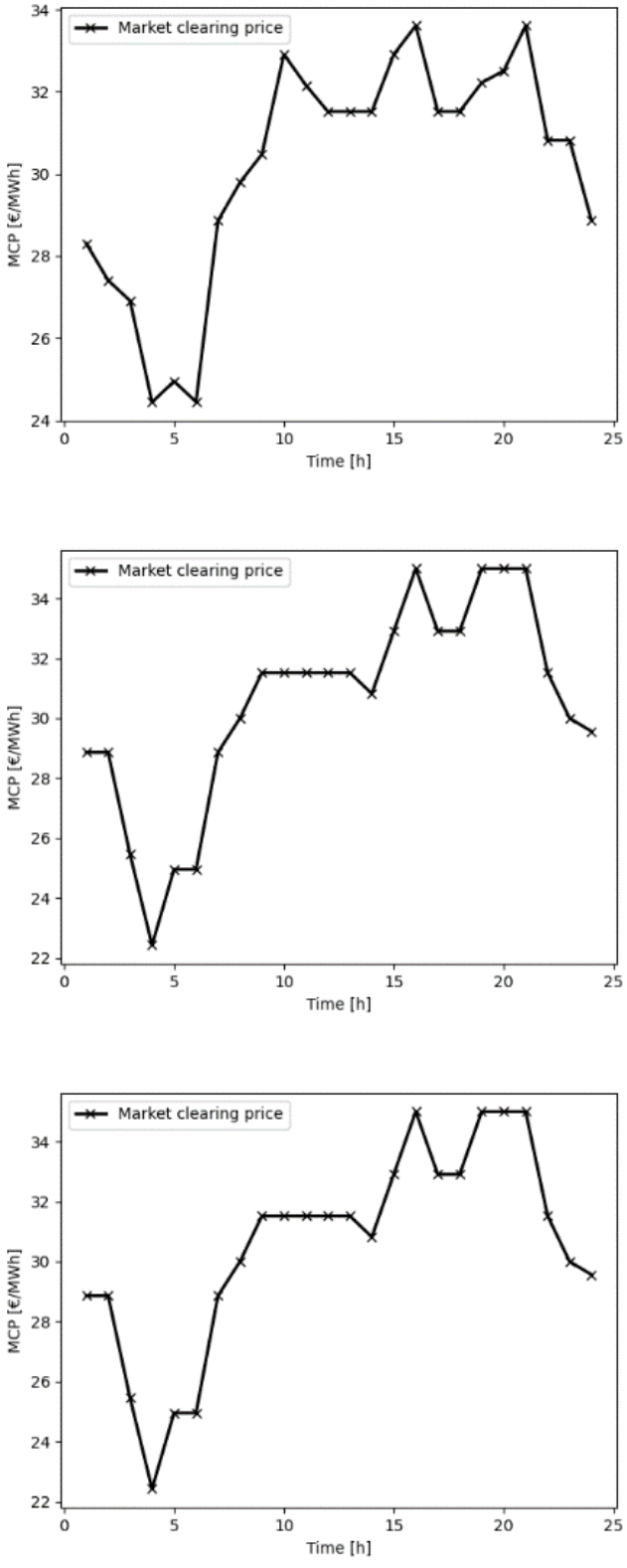

Figure B12– Market clearing price. In the top figure the availability cost of the storage is considered to be less than generator, in the middle figure the availability cost of storage and generators are equal and in the bottom figure the availability cost of storage is set to be less than the availability cost of the generator.

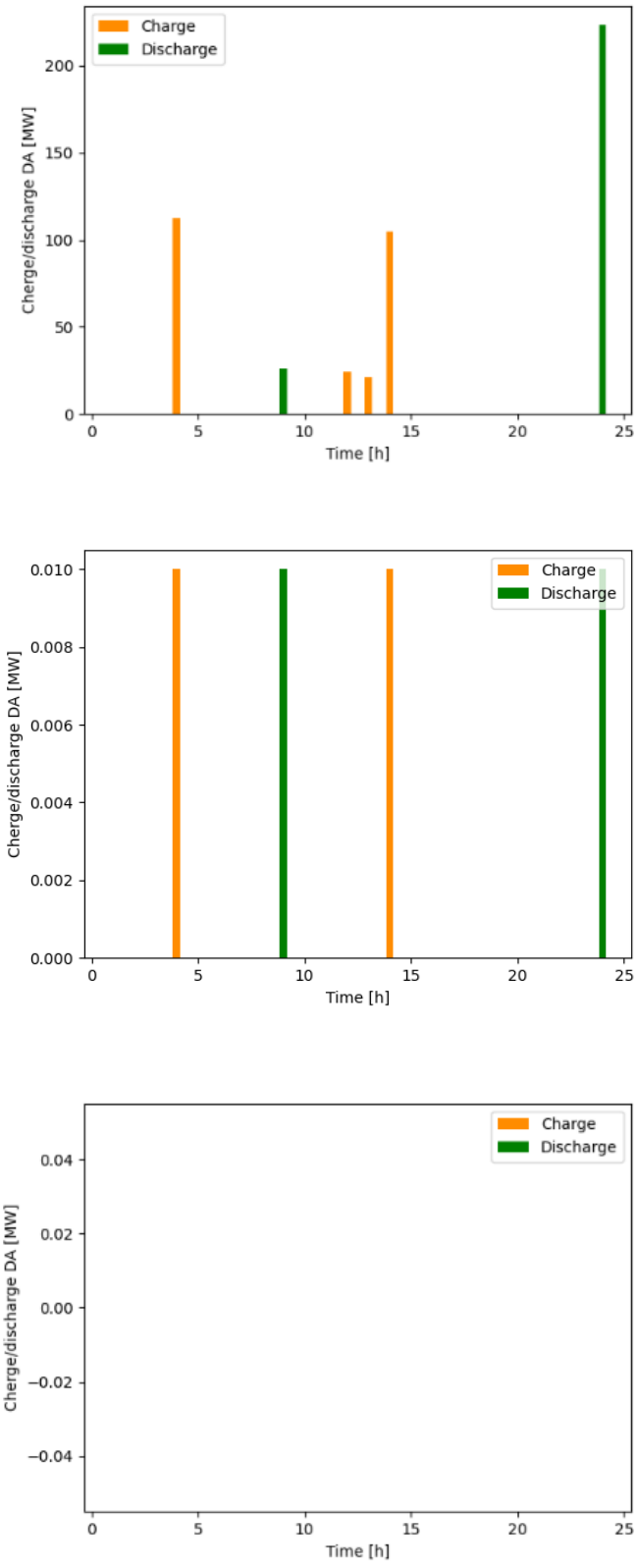

Figure B13– Day-ahead Charging and discharging of the storage. In the top figure the availability cost of the storage is considered to be less than generator, in the middle figure the availability cost of storage and generators are equal and in the bottom figure the availability cost of storage is set to be less than the availability cost of the generator.

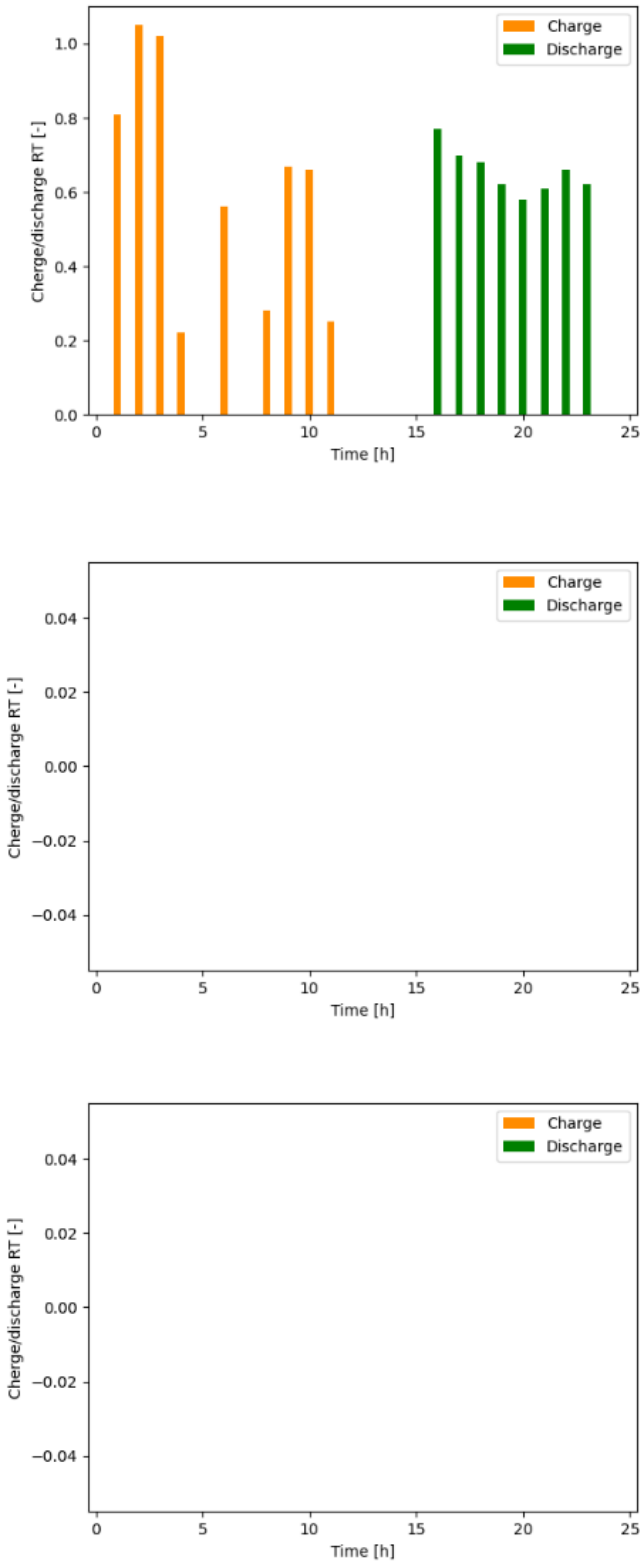

Figure B14– Real-time Charging and discharging of the storage. In the top figure the availability cost of the storage is considered to be less than generator, in the middle figure the availability cost of storage and generators are equal and in the bottom figure the availability cost of storage is set to be less than the availability cost of the generator.

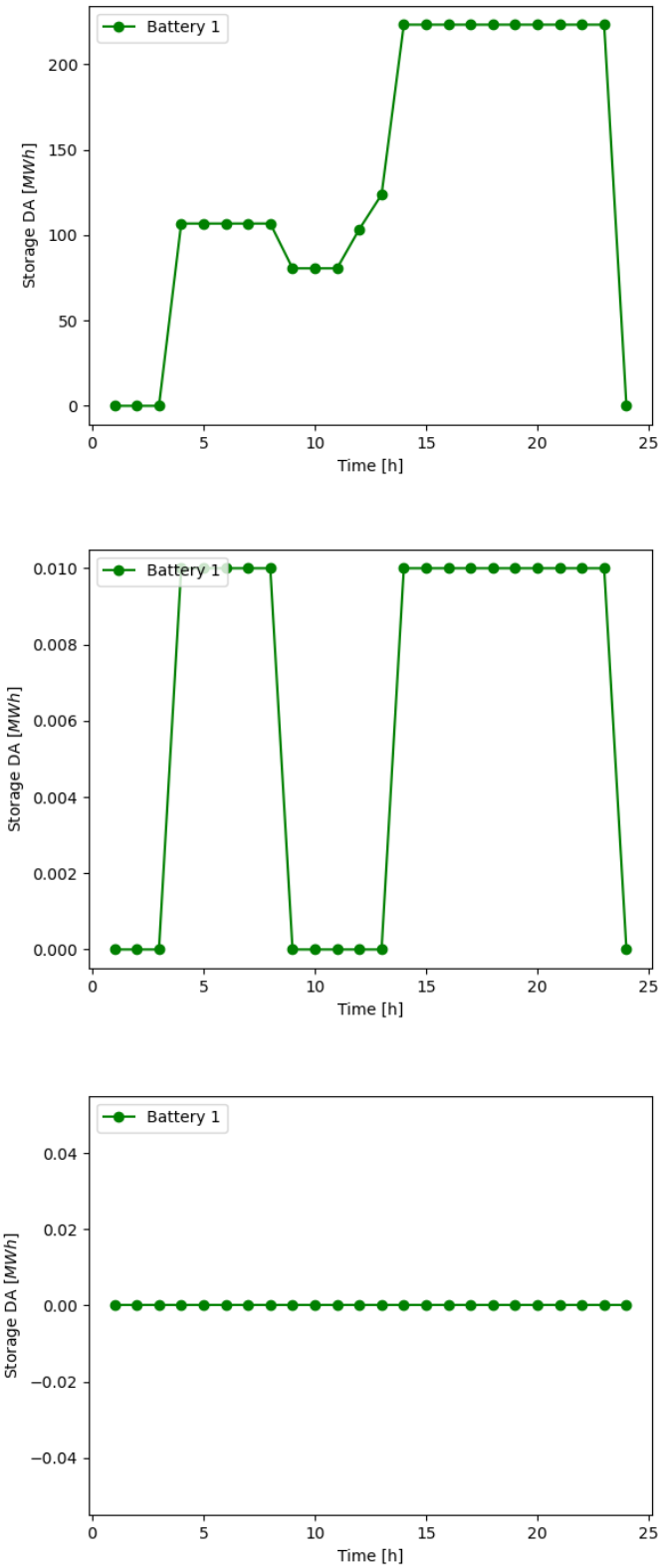

Figure B15– Storage energy state in day-ahead. In the top figure the availability cost of the storage is considered to be less than generator, in the middle figure the availability cost of storage and generators are equal and in the bottom figure the availability cost of storage is set to be less than the availability cost of the generator.

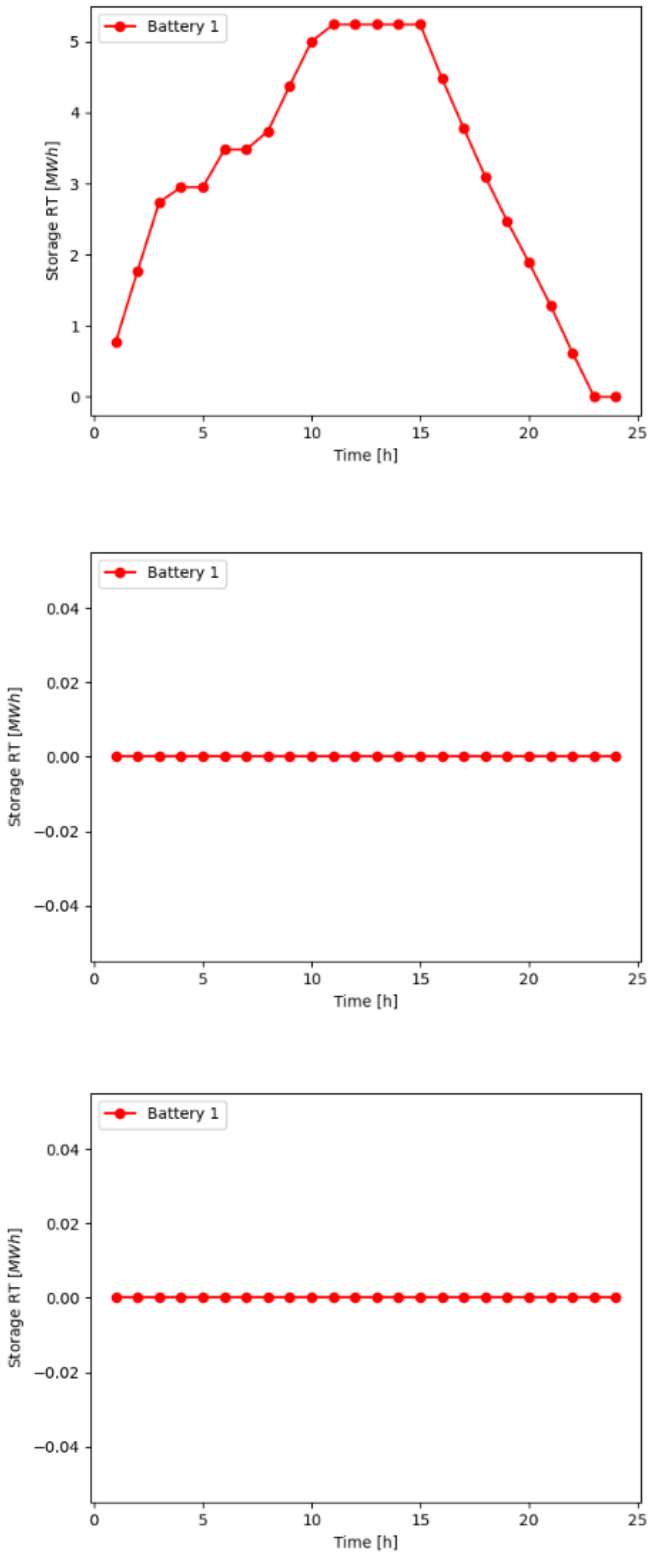

Figure B16– Storage energy state in real-time. In the top figure the availability cost of the storage is considered to be less than generator, in the middle figure the availability cost of storage and generators are equal and in the bottom figure the availability cost of storage is set to be less than the availability cost of the generator.

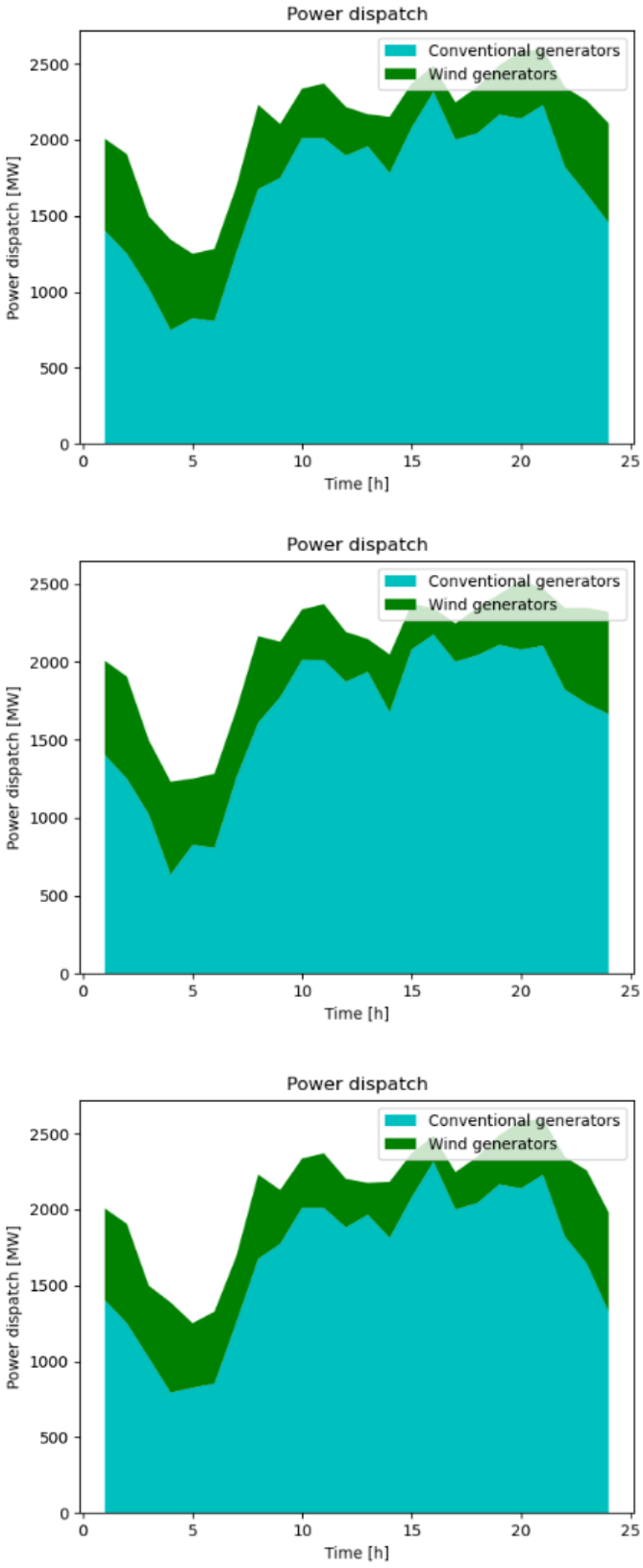

Figure B17– Scheduled DA power dispatch. In the top figure all the investment costs are set to 2€/MW, in the middle figure all the investment costs are set to 4€/MW, and on the bottom figure they are all set to 1€/MW.

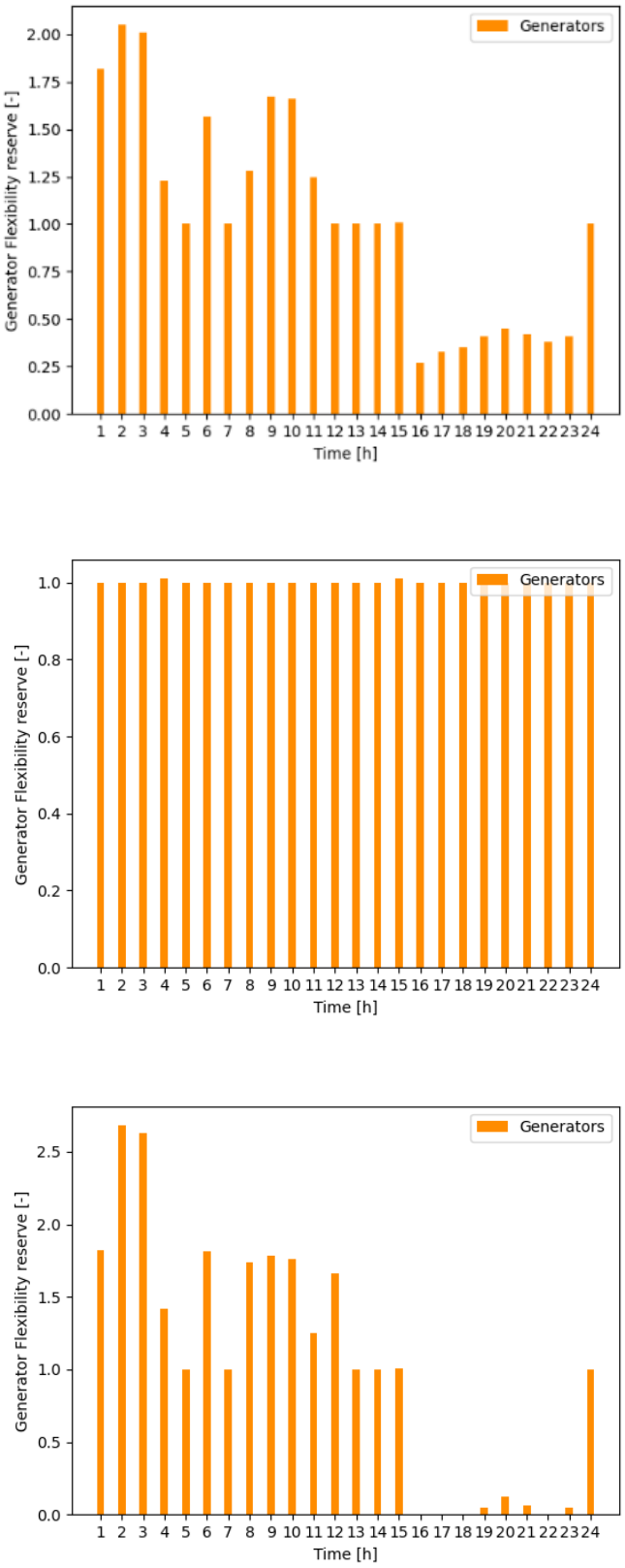

Figure B18– Generator Flexibility Reserve. In the top figure all the investment costs are set to 2€/MW, in the middle figure all the investment costs are set to 4€/MW, and on the bottom figure they are all set to 1€/MW.

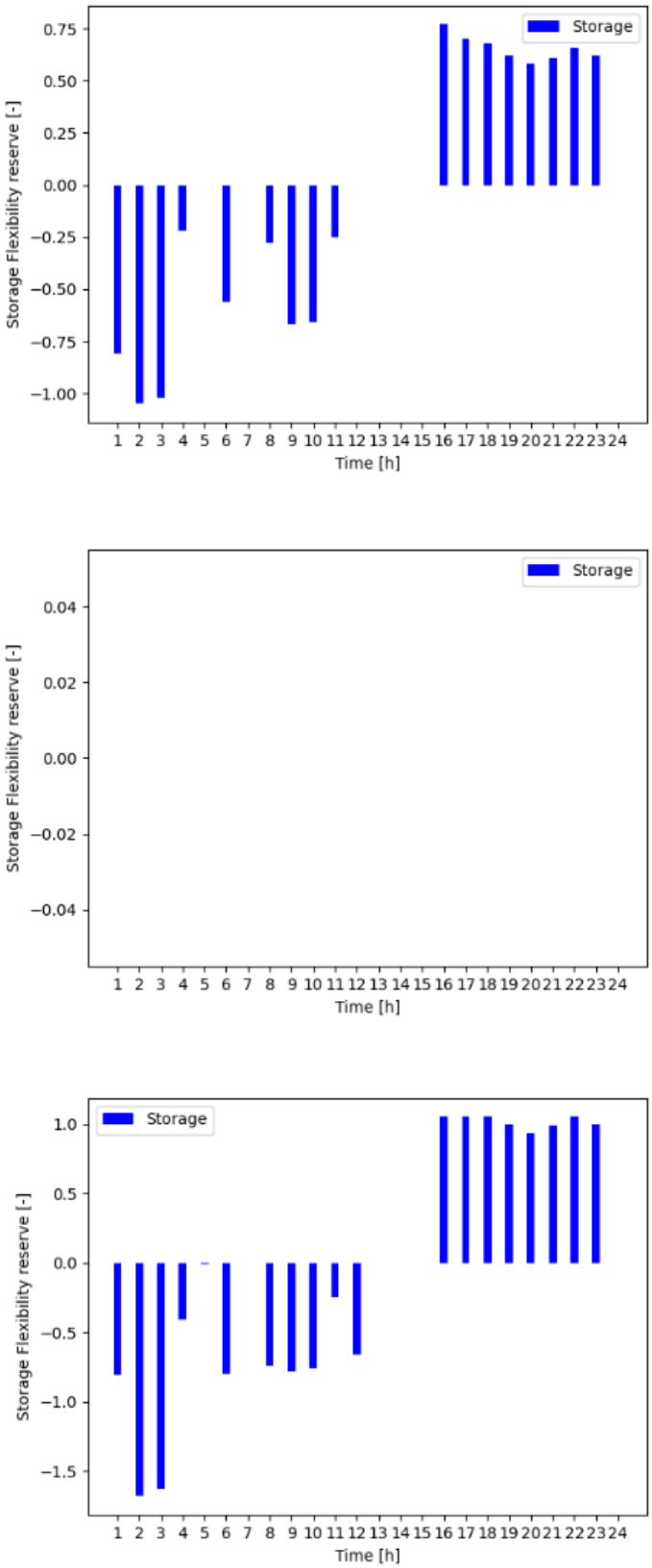

Figure B19– Storage Flexibility Reserve. In the top figure all the investment costs are set to 2€/MW, in the middle figure all the investment costs are set to 4€/MW, and on the bottom figure they are all set to 1€/MW.

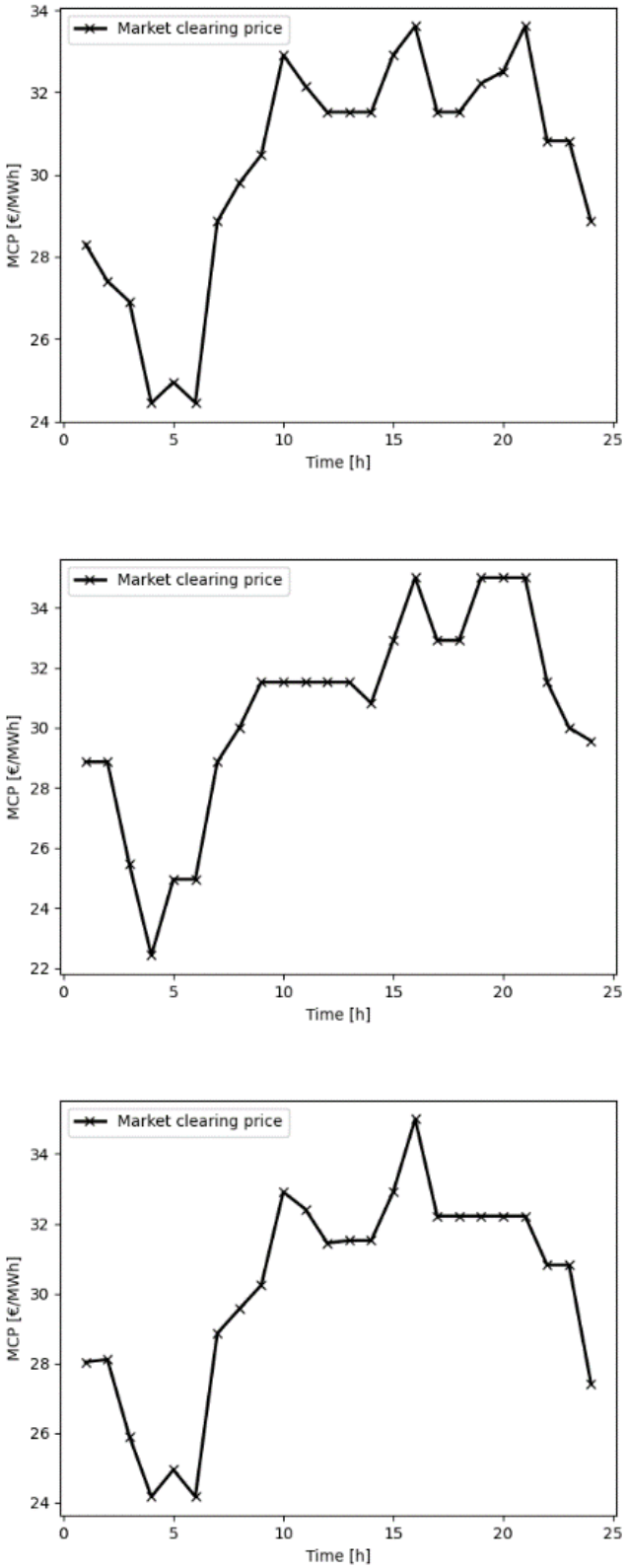

Figure B20– Market clearing price. In the top figure all the investment costs are set to 2€/MW, in the middle figure all the investment costs are set to 4€/MW, and on the bottom figure they are all set to 1€/MW.

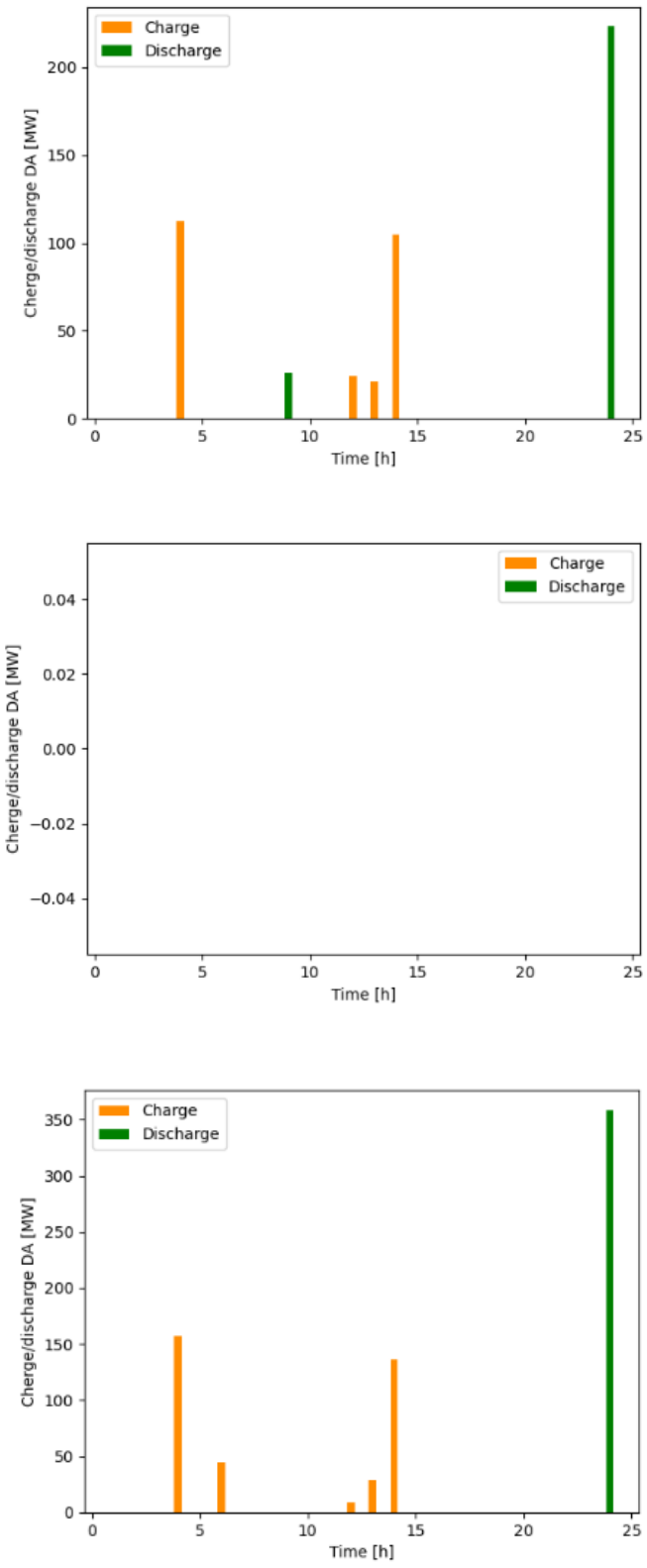

Figure B21– Day-ahead Charging and discharging of the storage. In the top figure all the investment costs are set to 2€/MW, in the middle figure all the investment costs are set to 4€/MW, and on the bottom figure they are all set to 1€/MW.

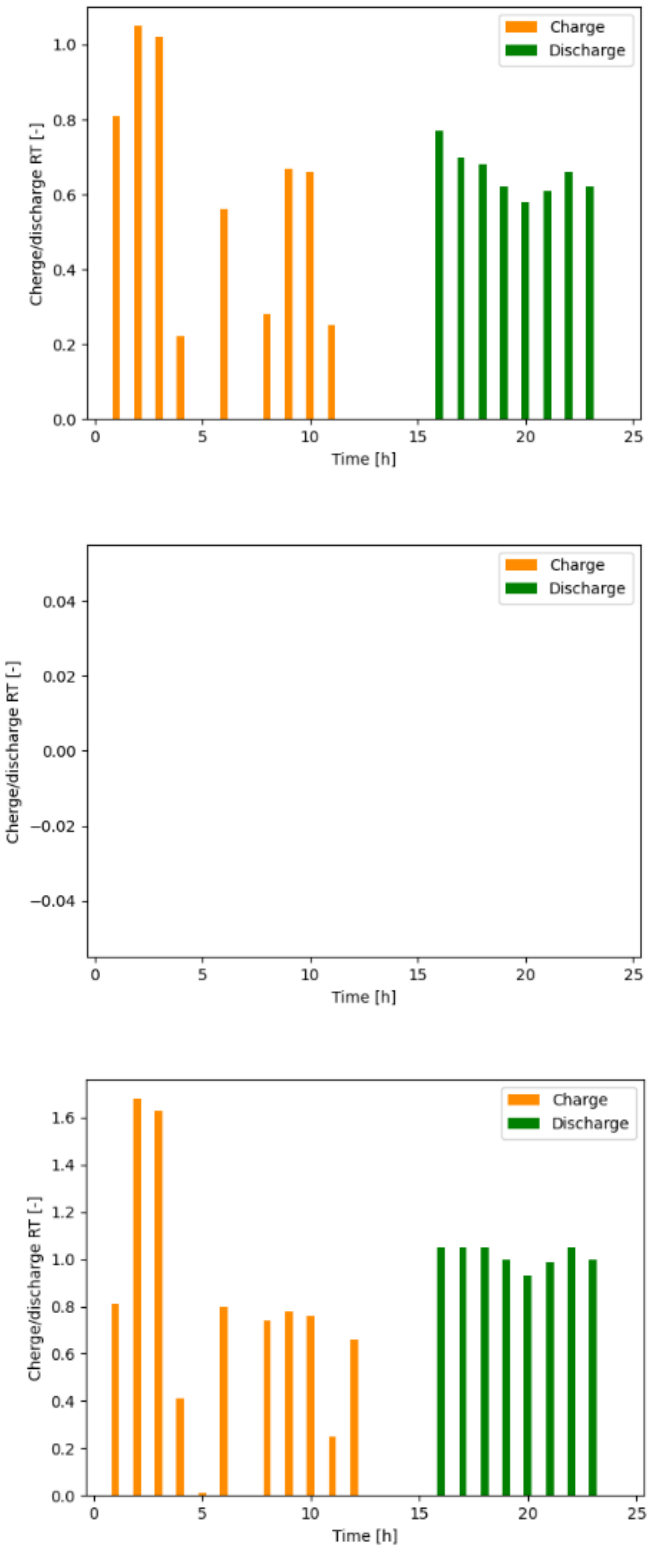

Figure B22– Real-time Charging and discharging of the storage. In the top figure all the investment costs are set to 2€/MW, in the middle figure all the investment costs are set to 4€/MW, and on the bottom figure they are all set to 1€/MW.

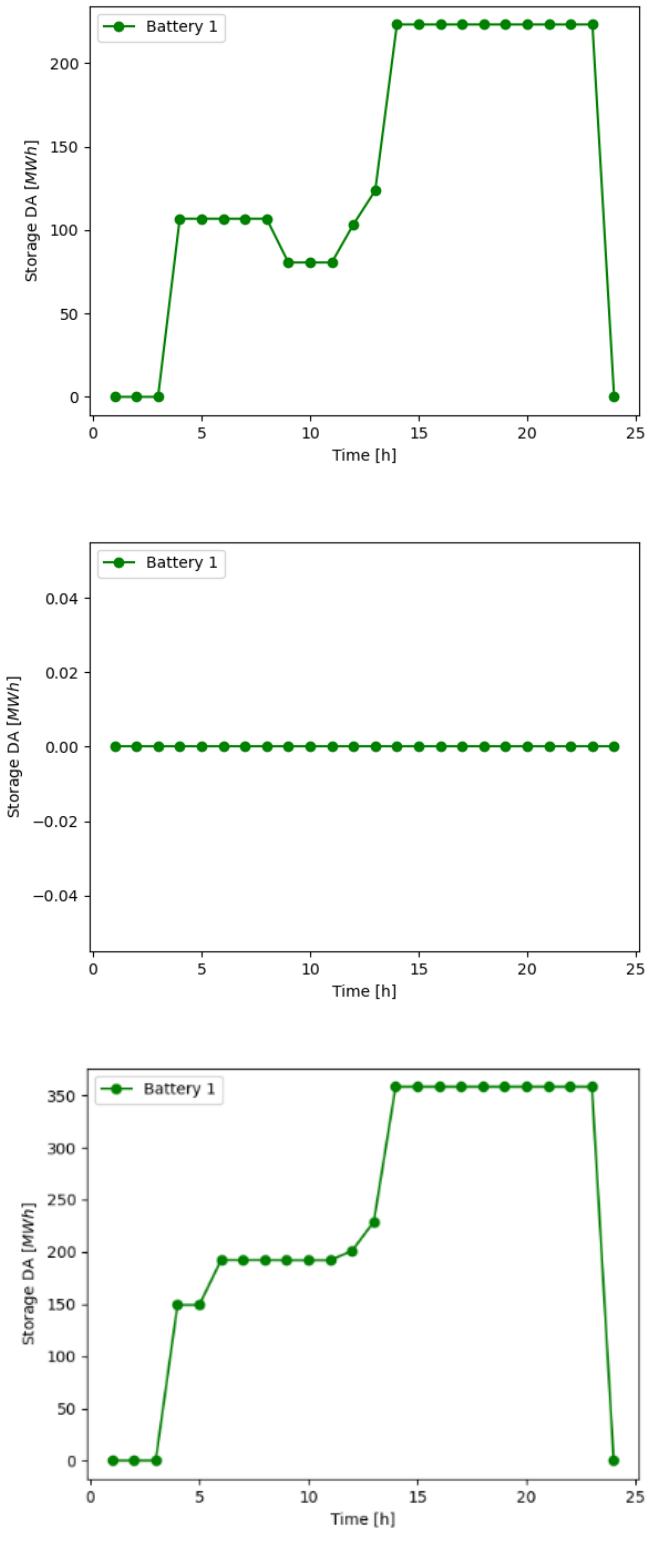

Figure B23– Storage energy state in day-ahead. In the top figure all the investment costs are set to 2€/MW, in the middle figure all the investment costs are set to 4€/MW, and on the bottom figure they are all set to 1€/MW.

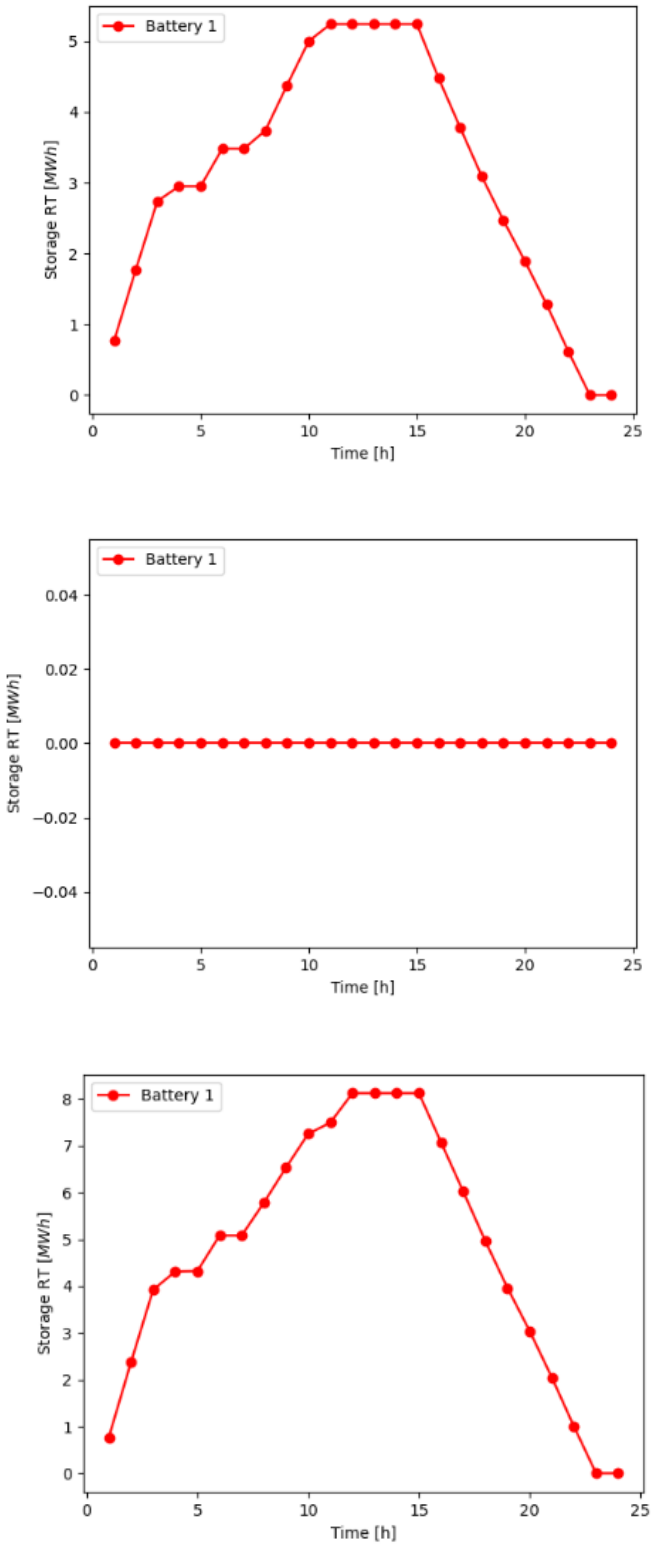

Figure B24– Storage energy state in Real-time. In the top figure all the investment costs are set to 2€/MW, in the middle figure all the investment costs are set to 4€/MW, and on the bottom figure they are all set to 1€/MW.